Forecasting Bike Sharing Demand Using Quantum Bayesian Network

Ramkumar Harikrishnakumar, Saideep Nannapaneni

Department of Industrial, Systems, and Manufacturing Engineering, Wichita State University, 1845 Fairmount St, Box 35, Wichita, KS, 67260 USA {rxharikrishnakumar@shockers.wichita.edu, saideep.nannapaneni@wichita.edu}

Corresponding author: Ramkumar Harikrishnakumar postal address: 1845 Fairmount St, Box 35, Wichita, KS, 67260 email:{rxharikrishnakumar@shockers.wichita.edu} Phone: +1 316-978-6240

Forecasting Bike Sharing Demand Using Quantum Bayesian Network

Abstract

In recent years, bike-sharing systems (BSS) are being widely established in urban cities to provide a sustainable mode of transport, by fulfilling the mobility requirements of public residents. The application of BSS in highly congested urban cities reduces the effect of overcrowding, pollution, and traffic congestion problems. The crucial role behind incorporating BSS depends on the prediction of bike demand across all the bike stations. The bike demand prediction involves real-time analysis for identifying the discrepancy between the bike pickup and drop-off throughout all the bike stations in a given time period. To enhance the prediction analysis of bike demand we propose quantum computing algorithms to provide computational speedup in comparison with classical algorithms. In this paper, we illustrate the construction of Quantum Bayesian Networks (QBN), for predicting bike demand. Furthermore, we provide a solution framework for implementing QBN for two case studies: (a) bike demand prediction during weekdays, (b) bike demand prediction during weekends. We have compared the quantum and classical solutions, by using IBM-Qiskit and Netica computing platforms.

Keywords: BSS, QBN, IBM-QISKIT, Demand prediction, Model averaging

1. Introduction

In recent times, the rapid spread of the coronavirus pandemic (COVID-19) have created unique challenges and affected the normal well-being of the economy, society, and public health systems by generating scenarios never seen before. The severity of the COVID-19 pandemic have drastically changed the public residents lifestyle and traveling choices by imposing stringent restrictions such as nationwide lockdown and traffic-control measures to reduce the spread of the pandemic (Villwock-Witte and van Grol, 2015; Krizek and Stonebraker, 2011; Lenton et al., 2008). Furthermore, through better air-flow ventilation, timely disinfection, and avoiding close proximity with travelers, the urban residents have adopted BSS as the alternative safe mode of public transport when compared to the use of subway in highly congested urban cities (Nikiforiadis et al., 2020; Cantelmo et al., 2020).

The Bike-sharing system is represented as a mobility service where bicycles are accessible to public residents for shared use. The bikes are available at a given station that are located all over the urban city areas and every station have the required number of docks. The residents can access the bikes from a given station location and are charged according to the bike usage duration. By engaging these bike-sharing systems the public transport administration will ensure a sustainable mode of transportation by reducing traffic congestion, pollution, carbon emission, and over-crowding problems in urban cities (He et al., 2018; Yang et al., 2020; Xie et al., 2023).

However, let us assume a scenario when the customer desired level of bike usage is observed in the early morning hours in a given dock station, then the demand for a number of bikes will change abruptly throughout the entire period because of uncertainty in the demand pattern. Fig.1 illustrates an overview of the BSS prediction problem. To resolve the bike-sharing demand problem, we need to make sure that supply bike stations satisfy predicted demand at any given location in real time. To, initiate this approach we have to focus on improving the computational aspect of the analysis using quantum computing

principles. Quantum technology has brought about a new paradigm shift in the computing platform by implementing fundamentals of quantum mechanics like entanglement, superposition, and measurement. The devices that have the potential to interpret classical information into the quantum paradigm are called quantum computing devices (McKay et al., 2018). The quantum computing devices manipulates the quantum mechanical phenomenon by storing the information in the units of qubit, which have the ability to store more information in comparison to classical qubits (Ajagekar et al., 2020; Qiskit Community, 2017). Quantum computing devices are categorized into two groups based on their system architecture: gate-based quantum devices and quantum annealing devices (Dallaire-Demers and Wilhelm, 2016; Osaba et al., 2022).

The gate-based quantum devices are represented by quantum gates to build the desired quantum circuits. Thereby, the quantum gates are applied to the individual qubit states to obtain the appropriate solution (Phillipson et al., 2022; Gyongyosi and Imre, 2019). Whereas, the quantum annealing devices are mainly used to solve NP-hard combinatorial optimization problems (Kadowaki and Nishimori, 1998). To evaluate the computational performance of gate-based and quantum annealing devices researchers have implemented these architectures in various complex domains to solve problems such as solving NPhard problem for identifying low cost nearest neighbour quantum circuits using harmony search heuristic algorithm (Alfailakawi et al., 2016), to mitigate fossil fuel consumption and environmental economic dispatch (EED) problem by using differential evolution crossover quantum particle swarm optimization (DE-CQPSO) algorithm (Xin-gang et al., 2020), to prioritize dynamic unpredictable events in a manufacturing shop floor using quantum firefly swarms for multimodal dynamic optimization (Ozsoydan and Baykasoğlu, 2019), to present data clustering technique using quantum chaotic cuckoo search algorithm (Boushaki et al., 2018), and to demonstrate smart rebalancing of bike sharing system under uncertainty using gate based quantum Bayesian network across three bike stations (Harikrishnakumar et al., 2021). However, in this work we have adopted

the gate based system architecture for representing the classical Bayesian network as Compositional Quantum Bayesian Network (C-QBN) due to its computational benefits for solving complex probabilistic problems such as bike demand forecasting.



Figure 1: Overview of BSS Prediction Problem

Primarily, Tucci (1995) implemented QBN as a quantum equivalent counterpart to the Bayesian network to enhance the overall performance of algorithms in comparison with classical counterparts such as Bayesian probabilistic models (Nielsen and Chuang, 2002; Kopczyk, 2018; Low et al., 2014; Woerner and Egger, 2019). Moreira and Wichert (2016) implemented a quantum-like Bayesian network for developing binary variable Bayesian networks by using heuristics techniques. Borujeni et al. (2021) proposed Compositional Quantum Bayesian Network (C-QBN) to represent a discrete Bayesian network using a quantum gate-based method. She et al. (2021) discussed the application of a Quantum-like Bayesian network by evaluating the interference between the attributes obtained from the multi-attribute decision-making (MADM) model. In this paper, we develop the Quantum Bayesian network by considering a generic 3-node Bayesian network with 2 states and also validate the results by implementing the circuit on a gate-based quantum platform.

Paper Contributions: The main technical contribution of this paper can be summarized as follows-(a) Developed an ensemble forecasting model with Long-short term memory (LSTM) and Gaussian process regression (GPR) as individual models whose results are aggregated using a Quantum Bayesian network, (b) The weights for the individual models are calculated as being inversely proportional to the root mean square error (RMSE) values, (c) Discretization of the continuous-valued bike demand forecasts to enable the construction of Quantum Bayesian networks, which can then be implemented on gate-based quantum computing platforms, (d) Simulated both the weekday and weekend QBN, using IBM Qiskit, (e) Validated the two Quantum Bayesian networks against classical Bayesian networks implemented using Netica.

Paper organization: The following paper is organized as follows with a bike demand prediction classification literature survey in Section 2. the background information of Bayesian networks, LSTM, and GPR models are presented in Section 3. A brief introduction to quantum circuits and quantum gates are provided in Section 4. Section 5 explains the construction of the Quantum Bayesian network. The methodology and framework of the proposed BSS forecasting model are explained in Section 6. The numerical results of the proposed approach are discussed in Section 7. Finally, Section 8 summarizes the conclusion and future work.

2. Literature Review

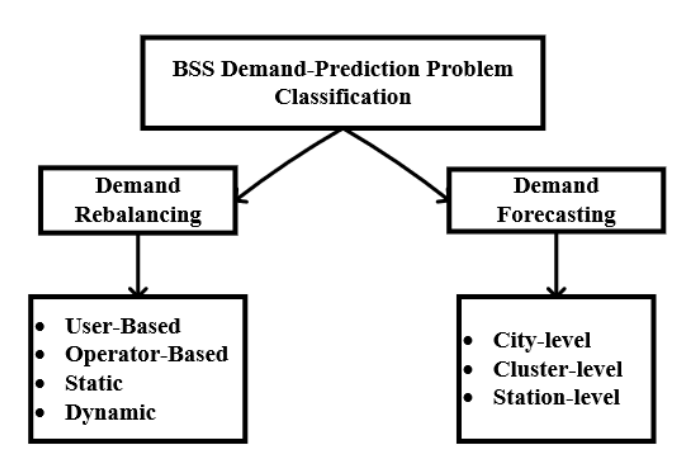


Figure 2: BSS Demand Prediction Classification (Cantelmo et al., 2020)

In recent years, many studies have considered bike-sharing systems as smart-mobility transportation models to provide sustainable public transport for mitigating traffic congestion and environmental pollution, and improving energy conservation in highly congested urban cities (Singhvi et al., 2015). Since, the BSS rental rates are subjected to temporal and spatial variations, the main challenge to operate BSS effectively depends on understanding the discrepancy between the supply-demand uncertainties (Lin et al., 2018; Caggiani et al., 2018).

To illustrate and solve the existing supply-demand uncertainties in BSS, the corresponding solution methods can be divided into two categories such as demand rebalancing and demand forecasting methods as shown in Fig2. In the former case of demand rebalancing, a redistribution strategy is applied to determine the number and location of bike stations for allocating bikes to the respective demand bike station. Furthermore, the rebalancing approach can be divided into the operator and user-based approaches. In an operator-based approach, a fleet of vehicle carriers are used to redistribute the bikes to the respective demand bike station, whereas, in the user-based approach, incentives are provided to rebalance the BSS.

The bike demand prediction methods can be classified as cluster-level, station levels, and city-level prediction problems (Xiao et al., 2020; Chai et al., 2018). Li et al. (2019) mentioned that city and cluster-level prediction models assist to merge stations as separate groups, to facilitate scheduling in the prediction process. Likewise, the station-level prediction model is unable to predict bike demand trends due to its dynamic nature. The external factors such as population, environmental factors, and work days contribute to the station-level bike prediction problem (Hulot et al., 2018). Chen et al. (2017) and Lin et al. (2018) proposed to implement deep neural network techniques to analyze the interactions between deep neural networks and linear regression model to forecast the hourly bike demand request at every station.

Dokuz (2021) proposed two novel algorithms to investigate the interest measures such as the frequency and continuity of bike usage frequency in Chicago

Divvy bike big datasets. The proposed approach predicts the frequency of daily bike usage in each of the bike stations and projects the overall demand across the complete divvy dataset. Xie et al. (2023) modeled the censored semi-bandit problem to optimize the number of pick-ups for multi-round bike demand allocation during unknown user demands. Ramesh et al. (2021) developed a real-time demand-supply prediction model using machine learning models such as random forest, linear regression, and boosting algorithms to forecast the bike demand at a given bike station during a specific time period. Erdoğan et al. (2014) implemented an integer programming model for static-bicycle relocation problems with demand intervals (SBRP-DI) to redistribute the bikes among the respective bike stations to minimize the overall relocation cost. Gammelli et al. (2022) presented a deep learning generative model by using a variational Poisson recurrent neural network (VP-RNN) to forecast the pick-up and drop-off of the bikes in the New York Citi-bike system. Li et al. (2023) utilized an irregular convolutional network (IrConv) model to forecast the correlation of bike usage amongst distant urban locations. The proposed model is evaluated and the model performance of bike stations is compared across five cities; New York, Chicago, Washington D.C., London, and Singapore respectively.

Recent studies have shown a great range of bike mobility prediction applications using graph theory and graph structures to analyze urban flows, spatiotemporal bike mobility patterns in different cities, urban traffic flow assessments, short-term bike demand forecasting, and examine urban travel flows in highly congested cities (Zaltz Austwick et al., 2013; Zhong et al., 2014). Yang et al. (2020) investigated the temporal transactions of bike traffic flows encoded in graphical structures for forecasting short-term BSS demand. Yang et al. (2019) examined the spatiotemporal bike flow patterns and graph-based approach to study the effect of mobility patterns, travel behaviors, and last-mile flow of the new metro line station in Nanchang, China. Zhang et al. (2017) utilized graph structure models to analyze spatiotemporal travel patterns for understanding traffic demand prediction.

Pan et al. (2019) proposed Long short-term memory, (LSTM) model for bike demand prediction during the bike renting and returning process and showed that the prediction model outperforms other deep learning models. Singhvi et al. (2015) mentioned the station-level demand prediction problem to examine the effect of influence factors like holidays, weekdays, weekends, traffic flow, and weather information for estimating bike demand prediction using regression models. Sathishkumar et al. (2020) used weather-related information along with bike-ridership data to predict the hourly rental bike demand using support vector machines, linear regression, and gradient boosting models. VE and Cho (2020) studied the impact of weather-related information in two bike data sets, Seoul bike data and capital bike share data for predicting bike demand using a rule-based regression model such as Classification and regression trees (CART), K-Nearest Neighbours (KNN), Randon forest, and conditional inference tree models. El-Assi et al. (2017) analyzed the effect of weather, socio-demographic, and environmental data to investigate the bike demand frequency of bike share in Toronto. Yu et al. (2022) proposed ensemble model using seasonal autoregressive integrated moving average (SARIMA) and long short-term memory (LSTM) models to predict and optimize bike relocation around urban rail transit station locations. Gao and Chen (2022) developed a machine learning model using KNN, random forest, SVM, and linear regression to study the performance of the demand prediction model under the influence of factors like weather information, traffic data, air pollution, and COVID-19 instances.

Ma et al. (2022) implemented a spatiotemporal graph attentional long-term short-term memory (STGA-LSTM) model to predict short-term bike demand from station-level using data sets from multiple sources. The (STGA-LSTM) model assists in extracting spatiotemporal information about bike mobility patterns and predicting the bike pick-up and drop-off demand patterns. Liu et al. (2019b) introduced two new methods using LSTM that can utilize multiple feature inputs and multiple time step outputs to enhance the accuracy of bike prediction in the first step and forecast the number of bikes in the second step.

Thereby assisting in better decision-making to relocate the bikes to the docker stations. Mehdizadeh Dastjerdi and Morency (2022) focuses on short-term bike demand forecasting in Montreal using LSTM deep learning approach. The proposed approach identifies six neighborhood communities using the Louvain algorithm along with four groups of LSTM to forecast the bike demand across the selected communities.

In addition, Gammelli et al. (2020) proposed censorship-aware demand modeling using the Gaussian process regression method to estimate latent demand of shared mobility during discrepancy in the supply. Cantelmo et al. (2020) implemented data mining techniques to retrieve bike demand patterns using the operational data of BSS. Likewise, Kaltenbrunner et al. (2010) also proposed data-mining methods to determine spatiotemporal bike demand patterns using the ARMA family of models and time series analysis. Additionally, machine learning techniques combined with data mining methods for predicting bike demands of dockless BSS (Ai et al., 2018; Liu et al., 2018). Zeng et al. (2016) utilized an ensemble approach using a gradient boosting decision tree (GBDT) and neural network methods to derive global features to enhance bike demand prediction. Kaspi et al. (2016) used probabilistic Bayesian network modelling to predict station bike demand using bike trip data. The above mentioned studies are summarized in Table 1 respectively.

However, after analyzing all the existing methods we can infer that the bike demand prediction requires real-time analysis to successfully predict the demand across the bike stations. This attempt is only possible by adopting an advanced computation platform that enables to increase in the efficiency and accuracy of prediction (Nielsen and Chuang, 2002). To enhance this new contribution, we previously proposed the C-QBN methodology approach and presented the theoretical framework for bike demand prediction (Harikrishnakumar et al., 2020). In this paper, we extend the proposed theoretical framework for New York Citi Bike datasets and validated the proposed quantum methods against classical Bayesian networks. We have included the following extensions as follows: (1)

Development of classical ensemble framework using Long-short term memory (LSTM) networks and Gaussian process regression (GPR) to represent Bayesian network for bike demand prediction; (2) Development of quantum circuit constructed by integrating conditional probabilities of Bayesian network; and (3) Illustration of the constructed QBN approach for predicting bike demand during weekdays and weekends of New-York citi-bike sharing systems. Hence, we implement the proposed solution approach for forecasting bike demand prediction. The proposed application of C-QBN for bike demand prediction can enhance other areas of Smart mobility in traffic monitoring, and vehicle incident prediction with a real-time solution by addressing these underlying issues related to transportation networks in urban cities.

3. Background Information

3.1. Bayesian Networks

Bayesian networks are probabilistic graphical model to represent uncertainty, evaluate risk and assist in decision making analysis. The Bayesian network is also known as directed acyclic graph, (DAG) that represents conditional probabilities with different variables of interest. The mathematical representation of Bayesian network is shown in Eq., 1. Now let us assume network with n nodes, where $\mathbb{Z} = \{Z_1, Z_2, ..., Z_n\}$ represents a set of nodes. Z_i represents parent node and node Z_j is called child node.

$$P(Z_1, Z_2, ..., Z_n) = \prod_{i=1}^n P(Z_i | \Pi_{Z_i})$$
 (1)

Where Π_{Z_i} represents parent nodes with respect to Z_i . The root nodes, $P(Z_i|\Pi_{Z_i})$ is equal to marginal probability distribution, $P(Z_i)$. The Fig.3 illustrates the Bayesian network of Two-node network. Where, A denotes root node and B represents the child node.

Work
Related
ž
$\ddot{\vdash}$
able
නි

			Chicago, U.S		Bari, I.T						Lyngby, D.K	Chicago, U.S	Beijing, C.N	D.C., USA						N.Y, Beijing	Seoul, K.R	Seoul, K.R	Toronto, C.A	Beijing, C.N	Seoul, K.R		Suzhou, C.N					
Methods	Arma, time Series Analysis Regression Applysis	RNN, LSTM	Multi-Graph Convolution NN	Random Forest, Gradient Boosted Tree	Non-linear Auto-regressive Networks	Graph Convolution Networks, GCN	LSTM, RNN	Attention-based Graph Model	Spatial & Temporal Clustering	Spatial-Temporal GCN	GPR, Bayesian Inference	Interest Measure Algorithm	Multi Armed Bandit Algorithm	RF, XG-Boosting, Linear Regression	VP-RNN deep learning model	IrConv deep learning model	Graph theory application	Graph theory applications	Graph theory applications	Deep residual networks	SVM, Boosted trees, Linear Regression	CART, KNN, CIT models	Multi-variable Regression Model	SARIMA & LSTM	KNN, Random Forest, SVM	STGA-LSTM deep learning model	LSTM deep learning model	LSTM deep learning model	Conv-LSTM model	Geo-CNN	GBDT & Neural Nets	Bayesian Inference Modelling QBN, LSTM, & GPR
Contribution	Investigate demand patterns to predict availability of blikes Predicting the bike usage during reak hours for Citi-bike RSS	Develop Recurrent networks to predict bike renting and returning demands	Develop multi-graph convolutional neural network model for demand prediction	Proposed model to predict station-level traffic for rebalancing BSS	Investigate free floating BSS for predicting bike demand over an operating area	Proposed GCN to predict station level demand in large scale BSS	Investigate to train LSTM model to predict bike pick-up and drop-off demands	Proposed spatial-temporal graph embedding to predict heterogeneous demand	Developed three-level data clustering to predict demand patterns	Proposed spatial-temporal GCN to predict pick up/drop-off demand	Developed censorship-aware modeling for bike demand prediction	Developed interest measure algorithm to predict the frequency of bike usage	Modelled censored semi-bandit problem for optimal bike demand allocation	Developed real-time demand-supply prediction model using ML models	Presented deep learning predictive model to forecast bike demand	Used IrConv deep learning model to forecast bike usage	Analyzed bike mobility prediction patterns across five cities	Examine spatial-temporal bike demand flow patterns	Forecast short-term bike demand using spatiotemporal bike flow patterns	Analyze Spatiotemporal patterns for crowd flow prediction	Proposed data mining techniques for bike demand prediction	Predicting bike demand using weather data	Study the effect of weather on Bike sharing demand	Predict & optimize bike relocation around transits stations	Developed ML models for bike demand predictions	Implement STGA-LSTM for predicting bike demand	Introduced multi-features LSTM model for bike demand prediction	Proposed short term demand forecasting using LSTM approach	Employed deep learning approach for forecasting bike demand	Proposed Geo-Convolution Neural nets (Geo-CNN) to predict bike demand	Presented Ensemble approach for bike demand prediction	Estimate the probability of unused bike count Developed novel Quantum Bayesian ensemble approach for bike demand prediction
Study	Singhti of al. (2010)	Chen et al. (2017)	Chai et al. (2018)	Hulot et al.(2018)	Caggiani et al. (2018)	Lin et al. (2018a)	Pan et al.(2019)	Li et al.(2019)	Cantelmo et al. (2020)	Xiao et al. (2020)	Gammellii et al. (2020)	Dokuz (2021)	Xie et al. (2023)	Ramesh et al. (2021)	Gammelli et al. (2022)	Li et al. (2023)	Zaltz et al. (2013)	Yang et al. (2019)	Yang et al. (2020)	Zhang et al. (2017)	Sathish et al. (2020)	Ve & Cho. (2020)	El-Assi et al. (2017)	Yu et al. (2022)	Gao & Chen (2022)	Ma et al. (2022)	Liu et al (2019b)	Mehdi et al. (2022)	Ai et al. (2018)	Liu et al. (2018)	Zheng et al. (2016)	Kaspi et al. (2016) This Study

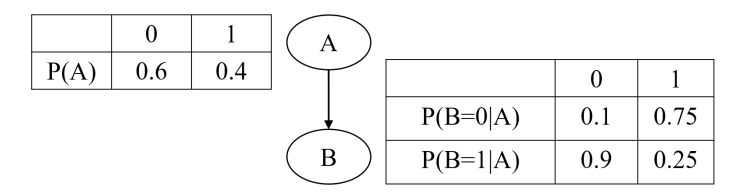


Figure 3: Illustration of Bayesian Network(Harikrishnakumar et al. (2020))

3.1.1. LSTM Model (Long short term memory neural network):

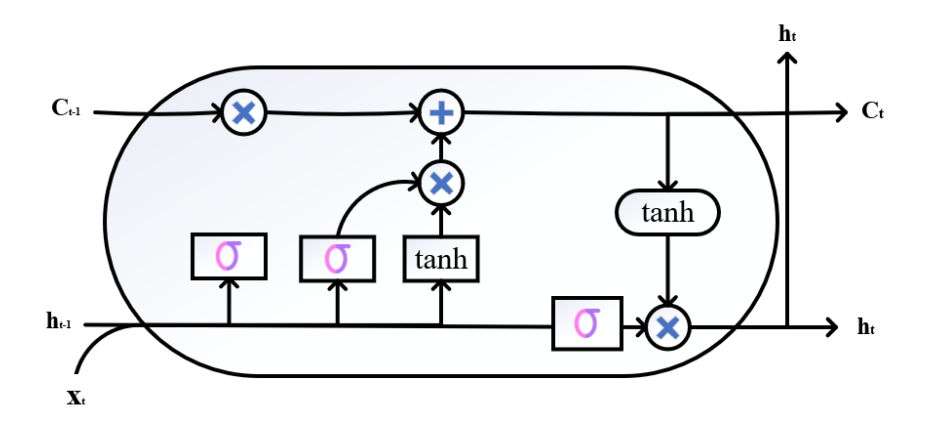


Figure 4: Illustration of LSTM network

LSTM is a variant of recurrent neural networks (RNN) used to process sequential data and memorize data from previous time steps for solving time series prediction problems (Goodfellow et al., 2016). The LSTM model is a different form of RNN which is capable of learning from long-time dependencies and also remain unaffected from vanishing gradient problem (Hochreiter and Schmidhuber, 1997). Fig.4 illustrates the complete mechanism and layers of LSTM model that consist of internal recurrence, self loop and an outer recurrence, that allows the network to store and update the information during the training process. Thereby, assisting the model to make predictions form the previous learning experiences (Wang and Kim, 2018). The mathematical expression of the LSTM model can be denoted as follows and the Eq.(2-7) are referenced as mentioned by Goodfellow et al. (2016):

$$f_t = (W_f[h_{t-1}, x_t] + b_t) (2)$$

$$i_t = \sigma(W_i[h_{t-1}, x_t] + b_i)$$
 (3)

$$\tilde{C}_t = tanh(W_c * [h_{t-1}, x_t] + b_c) \tag{4}$$

$$C_t = f_t \odot C_{t-1} + i_t \odot \tilde{C}_t \tag{5}$$

$$O_t = \sigma(W_o[h_{t-1}, x_t] + b_o) \tag{6}$$

$$h_t = O_t \odot tanh(C_t) \tag{7}$$

Where, t is the current time step, x is the input, o is the output, W is Weight matrix, b is bias. Accordingly, f_t , h_t , i_t , C_t are four intermediate parameters that store and remember the input data, while σ is sigmoid activation function and tanh denotes the hyperbolic tangent activation function respectively. The LSTM model proposed in this paper consist of two input LSTM layers and the output layer would make the final predictions of bike-sharing demands across bike station during weekdays and weekends of New York Citi-Bike stations.

3.1.2. Gaussian Process Regression Model:

Gaussian process regression (GPR) is an extremely useful tool which belongs to the field of probabilistic machine learning method to perform non-parametric regression with the Gaussian process (Rasmussen and Nickisch, 2010). For instance, given a dataset $D = (x_i, y_i)$ with n input vectors x_i and output vectors y_i , the corresponding probability distribution over the function f(x) follows a Gaussian distribution as follows:

$$f(x) \sim GPR(m(x), k(x, x')) \tag{8}$$

The Gaussian process models this distribution by means of multivariate Gaussian distribution using the mean function m(x) and co-variance function k(x,x') expressed as follows:

$$m(x) = E(f(x)) \tag{9}$$

$$k(x, x') = E[(m(x) - f(x'))(m(x) - f(x'))]$$
(10)

where, E is the expectation value and k(x,x') is the kernel function that provides the relation between the training dataset and the predicted target output. In solving a regression problem the target output y is expressed by prior distribution as:

$$y \sim N(0, K(x, x') + \sigma_n^2 I_n)$$
 (11)

While performing the Gaussian distribution between the testing set $x^{'}$ and training set x, the predicted output $y^{'}$ is set to follow a joint prior distribution with the target output y as follows:

$$\begin{bmatrix} y \\ y' \end{bmatrix} \sim N(0, \begin{bmatrix} k(x,x) + \sigma_n^2 I_n & k(x,x') \\ k(x,x')^T & k(x',x') \end{bmatrix}$$
(12)

N represents normal distribution, σ_n is the noise level term, k(x,x'), k(x',x') is the co-variance matrices of the training and testing sets, and covariance matrix k(x,x) is defined as:

$$k(x,x) = \begin{bmatrix} k(x_1, x_1) & k(x_1, x_2) & \dots & k(x_1, x_n) \\ \vdots & \vdots & \dots & \vdots \\ k(x_n, x_1) & k(x_n, x_2) & \dots & k(x_n, x_n) \end{bmatrix}$$
(13)

The squared exponential kernel function is also called as radial basis function (RBF) and represented as:

$$k(x, x') = p_1 * exp(-\frac{(x - x')^2}{2 * p_2})$$
(14)

The hyper-parameters p_1 represent the amplitude of the covariance, and p_2 represent the length scale parameters which represent the correlation between

the highly spread points. After, performing the Gaussian distribution it is necessary to measure and validate the performance of the GPR, by optimizing the hyper-parameter p_1 and p_2 in the co-variance function during the training process (Liu et al., 2019a). Finally, after optimizing the hyper-parameters of GPR, the predicted target output y' can be derived by calculating the conditional probability distribution p(y'|x',x,y) as follows:

$$p(y'|x', x, y) \sim N(y'|\bar{y'}, cov(y'))$$
 (15)

Where, $\bar{y'}$ represents mean values of the predicted output and cov(y') is the co-variance matrix that measures the uncertainty in the predictions.

4. Quantum circuits and Quantum Gates

Quantum computation involves the manipulation of quantum systems used to process quantum information. The generic computational basis of a quantum system can be represented as:

$$|\psi\rangle = \alpha |0\rangle + \beta |1\rangle \tag{16}$$

In the quantum system mentioned in Eq. 16, the two systems; $|0\rangle$ and $|1\rangle$ are the basic unit of computation for two-qubit system given in vector form such as;

$$|0\rangle = \begin{bmatrix} 1\\0 \end{bmatrix} |1\rangle = \begin{bmatrix} 0\\1 \end{bmatrix} \tag{17}$$

The states in Eq. 17 are similar to classical binary bits 0 and 1 used in classical systems. However, the classical bits are different from qubits due to the principle of superposition between both states $|0\rangle$ and $|1\rangle$ respectively. These qubits are used to execute quantum calculations which is accomplished by performing series of fundamental mathematical operations called as Quantum logic gates. These quantum gates are represented by an operator that transforms to

map one quantum state into another quantum state (Nielsen and Chuang, 2002). Here, we discuss single and multi-qubit gates to construct quantum circuit using QBN approach.

4.1. Single and Multi-Qubit Gates:

The gates Hadamard (H), Pauli-X, Identity (I), and Pauli-Z are denoted by the unitary operators that are represented in matrix form as shown below:

$$H = -\begin{bmatrix} H \end{bmatrix} - \begin{bmatrix} 1 & 1 \\ 1 & -1 \end{bmatrix} \qquad Pauli - X = -\begin{bmatrix} X \end{bmatrix} - \begin{bmatrix} 0 & 1 \\ 1 & 0 \end{bmatrix}$$

$$I = -\begin{bmatrix} I - 0 \\ 0 & 1 \end{bmatrix} \qquad Pauli - Z = -\begin{bmatrix} Z - 0 \\ 0 & -1 \end{bmatrix}$$

Figure 5: Matrix form of H, X, I, Z Gates

The Hadamard gate or H-gate plays a critical role in quantum computing systems, which assists in transforming a qubit from one computational basis to a superposition of two states (Santos, 2016; Qiskit Community, 2017). The Hadamard gate represents the possible combination of all the states of qubits given in a quantum circuit. For instance in 2-qubit quantum system, $|\Psi_0\rangle$ where $|\Psi_0\rangle = a_0 |00\rangle + a_1 |01\rangle + a_2 |10\rangle + a_3 |11\rangle$, the possible combination of quantum states are $2^2 = 4$. Hence, the resulting superposition of states when Hadamard gate is applied to states $|0\rangle$ and $|1\rangle$, is shown below:

$$H|0\rangle = \frac{1}{\sqrt{2}} \begin{bmatrix} 1 & 1\\ 1 & -1 \end{bmatrix} \times \begin{bmatrix} 1\\ 0 \end{bmatrix} = \frac{|0\rangle + |1\rangle}{\sqrt{2}}$$
 (18)

$$H|1\rangle = \frac{1}{\sqrt{2}} \begin{bmatrix} 1 & 1\\ 1 & -1 \end{bmatrix} \times \begin{bmatrix} 0\\ 1 \end{bmatrix} = \frac{|0\rangle - |1\rangle}{\sqrt{2}}$$
 (19)

The X-gate flips the states of the qubit, the state $|0\rangle$ to $|1\rangle$ and $|1\rangle$ to $|0\rangle$. The X-gate operator flips the input state of the qubits as follows:

$$X|0\rangle = \begin{bmatrix} 0 & 1\\ 1 & 0 \end{bmatrix} \times \begin{bmatrix} 1\\ 0 \end{bmatrix} = \begin{bmatrix} 0\\ 1 \end{bmatrix} = |1\rangle \tag{20}$$

$$X|1\rangle = \begin{bmatrix} 0 & 1\\ 1 & 0 \end{bmatrix} \times \begin{bmatrix} 0\\ 1 \end{bmatrix} = \begin{bmatrix} 1\\ 0 \end{bmatrix} = |0\rangle \tag{21}$$

The Z-gate is a unitary gate that is referred as phase-flip operator as it maps 1 to -1 as it flips the phase of the qubits and leaves the state $|0\rangle$ unchanged (Qiskit Community, 2017), whereas the Z-gate transforms $|1\rangle$ to $|-1\rangle$ as shown below:

$$Z|0\rangle = \begin{bmatrix} 1 & 0 \\ 0 & -1 \end{bmatrix} \times \begin{bmatrix} 1 \\ 0 \end{bmatrix} = \begin{bmatrix} 1 \\ 0 \end{bmatrix} = |0\rangle$$
 (22)

$$Z|1\rangle = \begin{bmatrix} 1 & 0 \\ 0 & -1 \end{bmatrix} \times \begin{bmatrix} 0 \\ 1 \end{bmatrix} = \begin{bmatrix} 0 \\ -1 \end{bmatrix} = |-1\rangle$$
 (23)

4.2. Rotational Gates:

$$|q_0\rangle$$
 — $R_x(\phi_1)$ — $R_y(\phi_2)$ —

Figure 6: Illustration for Qubit Rotation Bergholm et al. (2018)

For qubit rotation Bergholm et al. (2018), implement the qubit on the ground state $|0\rangle$ and apply rotation around-x axis as shown below:

$$R_x(\phi_1) = e^{-i\phi_1\sigma_x/2} = \begin{bmatrix} \cos(\phi_1/2) & -i\sin(\phi_1/2) \\ -i\sin(\phi_1/2) & \cos(\phi_1/2) \end{bmatrix}$$
(24)

Here, we apply the rotation gate around y-axis as shown in Eq. 24:

$$R_y(\phi_2) = e^{-i\phi_2\sigma_y/2} = \begin{bmatrix} \cos(\phi_2/2) & -\sin(\phi_2/2) \\ \sin(\phi_2/2) & \cos(\phi_2/2) \end{bmatrix}$$
 (25)

After, applying the rotation along the x and y axis, the corresponding qubit state is denoted as:

$$|\psi\rangle = R_y(\phi_2)R_x(\phi_1)|0\rangle \tag{26}$$

Finally, we apply the rotation along the Z-axis using the Pauli-z operator, σ_z and based on the parameters of ψ_1 and ψ_2 the qubit state lies between $1(\psi=|0\rangle)$ and $-1(\psi=|1\rangle)$ and the corresponding qubit state is denoted as follows:

$$\langle \psi | \sigma_z | \psi \rangle = \langle 0 | R_x(\phi_1)^* R_x(\phi_2)^* \sigma_z R_x(\phi_2) R_x(\phi_1) | 0 \rangle \tag{27}$$

4.3. Multi-Qubit Gates:

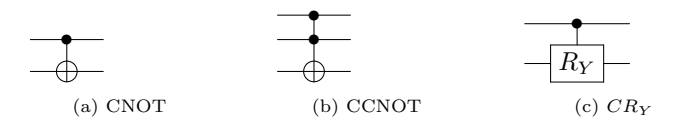


Figure 7: Representation of Multi-qubit gates

In this section we discuss the multi-qubit gates CNOT, CCNOT gate and CR_y gates as shown in Fig. 7. The CNOT gate is denoted as controlled-NOT gate or Feynmann gate. In general, the CNOT gate has one control qubit and one target qubit. Whereas, the CCNOT gate is also denoted as toffoli-gate and in the case of CCNOT gate both the control qubits are in state $|1\rangle$ and we apply X-gate to the target qubit. In case of CR_y gate we apply rotation, R_y during control qubits is $|1\rangle$ state. Hence, in a quantum circuit involving multiqubit gates can be decomposed into a series of single qubit gates and CNOT gates. To, provide the computational basis when executed on actual quantum hardware (Nielsen and Chuang, 2002).

5. Constructing of QBN circuit

In this section, we illustrate the Bayesian network in quantum paradigm inspired from Borujeni et al. (2021). Here, we present crucial steps to construct the quantum circuit for a Bayesian network:

- Relate each of node of the Bayesian network to the respective number of qubits based on the discrete state of the nodes.
- 2. Outline the conditional probabilities of every node of Bayesian network to the corresponding probability or probability amplitudes of qubit states.
- 3. Obtain the probability amplitudes of the associated quantum states by applying CR_y rotational gates.

From, the above mentioned principles regarding the construction of Quantum Bayesian network we can develop a quantum circuit for two node Bayesian network in Fig. 3. The nodes in the Bayesian network shown in Fig.3 consist of two states 0 and 1, we can relate state 0 and state 1 of the Bayesian nodes to the corresponding qubit states $|0\rangle$ and $|1\rangle$. The two nodes A and B can be related to two qubits q_0 and q_1 . For qubits q_0 and q_1 we need to provide controlled rotation gates CR_y with angles θ_A and θ_B respectively. By doing so, we can map the conditional probabilities of the nodes A and B to the corresponding probabilities of the quantum states q_0 and q_1 . Thereby, resulting in two rotation values from its parent node, A. The two rotation for node B, $(\theta_{B,0})$ and $(\theta_{B,1})$ illustrating its probabilities for A=0 and A=1. The controlled rotation is applied when the control qubit is in $|1\rangle$ state. The conditional probabilities are obtained when the parent node, (A) value is 0. This is when we apply the X-gate as flip operator to transform state $|0\rangle$ to state $|1\rangle$. In Fig.3, there is one parent node, A and we apply CR_y gate to obtain the conditional probabilities of the parent node, A. For instance, when there are n parent nodes then the resulting controlled rotation gate will be $C^n R_y$ gate.

In Fig. 3, the parent node, A can be represented using a single qubit gate. The probability of the parent node can be related to the probability amplitudes of the States $|0\rangle$ and $|1\rangle$ by providing CR_y gate with a desired rotation. After, the application of the CR_y , the ground state of qubit is transformed as follows:

Ground state,
$$|0\rangle = \cos\theta |0\rangle + \sin\theta |1\rangle$$
 (28)

Where, θ denotes the angle of rotation corresponding to parent node. The probabilities are denoted by $\cos^2(\theta/2)$ and $\sin^2(\theta/2)$ for the states $|0\rangle$ and $|1\rangle$.In Eq.29 (θ_A) denotes The angle of rotation is obtained as follows:

$$\theta_A = 2 \times \tan^{-1} \sqrt{\frac{P(|1\rangle)}{P(|0\rangle)}} = 2 \times \tan^{-1} \sqrt{\frac{P(A=1)}{P(A=0)}}$$
 (29)

The Fig.8 illustrates the schematic illustration of quantum circuit with series of single qubits and rotation angles of two node Bayesian network.

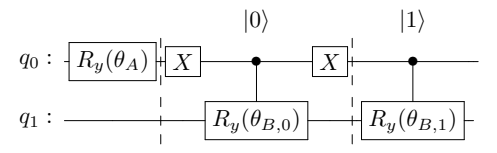


Figure 8: Representation of QBN circuit for two-node network in Fig. 3Harikrishnakumar et al. (2020)

In the case, where n represents counts of parent nodes and when parent node counts are more than 1. During, such a scenario, the probabilities of the child node are obtained by applying controlled rotation, $(C^nR_y(\theta))$. To, implement $(C^nR_y(\theta))$ gate we need to apply dummy qubits or ancilla qubits (Nielsen and Chuang, 2002). The C^nR_y gate requires (n-1) ancilla qubits, by doing so the C^nR_y gate can be decomposed into series of 2(n-1) CCNOT gate, and one CR_y gate respectively. Fig. 9, illustrates multi-qubit gate C^4R_y , In the following circuit, 4 control qubits and 3 ancilla qubits are required to decompose the multi-qubit gate using a combination of single qubit gates and CNOT gates.

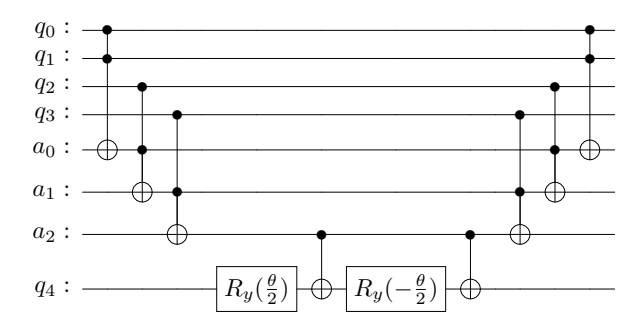


Figure 9: Ancilla qubit gates representing $C^4 R_y$ gate Harikrishnakumar et al. (2020)

If a variable in Bayesian network have more than two states. The qubit representation of the discrete variable is given as $\lceil \log_2 n \rceil$, where n denotes various states of the variable. During such a scenario, transformation U-gate is implemented for qubits of the corresponding variable in Bayesian network.

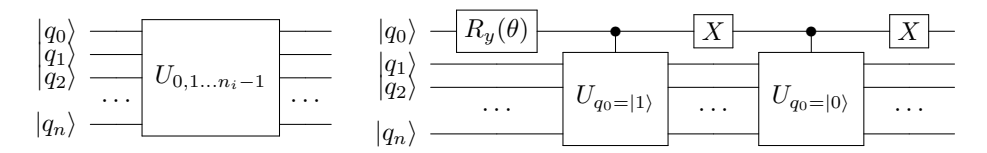


Figure 10: U-gate Transformation for a variable with more than two states Harikrishnakumar et al. (2020)

The transformation U-gate, with appropriate angle of rotations will transform the qubits to get required probabilities. Fig. 10 depicts a scenario in Fig.3 when variable B have more than two states. In such a scenario, U-gate is decomposed into series of single qubit gates.

6. Methodology

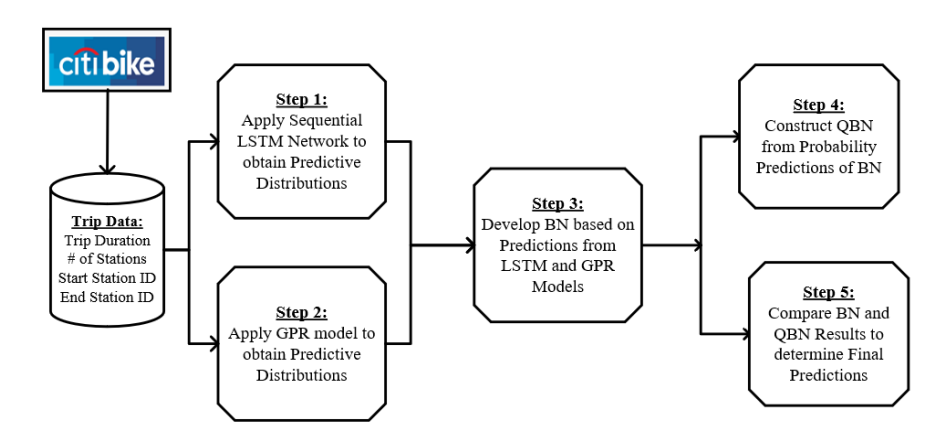


Figure 11: Methodological Framework of the Proposed BSS Forecasting Approach

To accomplish a multi-dimensional perspective of the spatio-temporal predictions of bike sharing system, a framework model is proposed to forecast the bike predictions during different spatial and temporal periods. The proposed framework encompasses (i) a deep learning technique using Long short term memory, (LSTM) for better classifying, processing and predictions based on the time-series data to understand the entire dynamics of the system, (ii) the Gaussian process regression, (GPR) model to interpret the shared mobility predictions during different spatial and temporal scales, (iii) an ensemble method of Bayesian Network, (BN) and Quantum Bayesian network, (QBN) to perform uncertainty propagation to overcome the uncertainties in bike demand forecasting, (iv) finally a set of visualization tools for illustrating the results of bike demand predictions. A schematic illustration of the proposed approach is shown in Fig. 11.

In the proposed approach, the raw data, which includes trip durations, starting and ending geographical locations of bike stations. The dataset obtained are initially preprocessed to make sure that there are no imperfections in the data such as redundancies and missing information in the data that can affect the overall performance of the model.

Considering the broad scheme of variables contributing to bike sharing demands, we mainly focus on predicting the availability of bike counts in the respective station locations throughout the day during weekdays and weekends. By doing so we are able to investigate on the dynamic aspect of bike demand prediction in a real-time world scenario. A LSTM model is adopted to study the bike mobility modelling during different time intervals and its impact over a specific bike location zone. GPR, a supervised learning algorithm used for regression and probabilistic classification problems is also used in this context. A non-parametric machine learning model used for modelling spatial and time-series data, makes GPR a robust technique for incorporating non-linear and complex data. Furthermore, visualization tools such as spatio-temporal heatmap, bubble-map showing high intensity bike demand locations, and box-plots of average bike counts during weekdays and weekends are designed to provide appropriate information regarding the associated spatial and temporal bike de-

mand patterns.

6.1. Data-set Description:

In order to validate the effectiveness of the proposed prediction model, we verify it based on the bike-sharing system of New York City (NYC) and compare the results with the proposed methods obtained in this section.

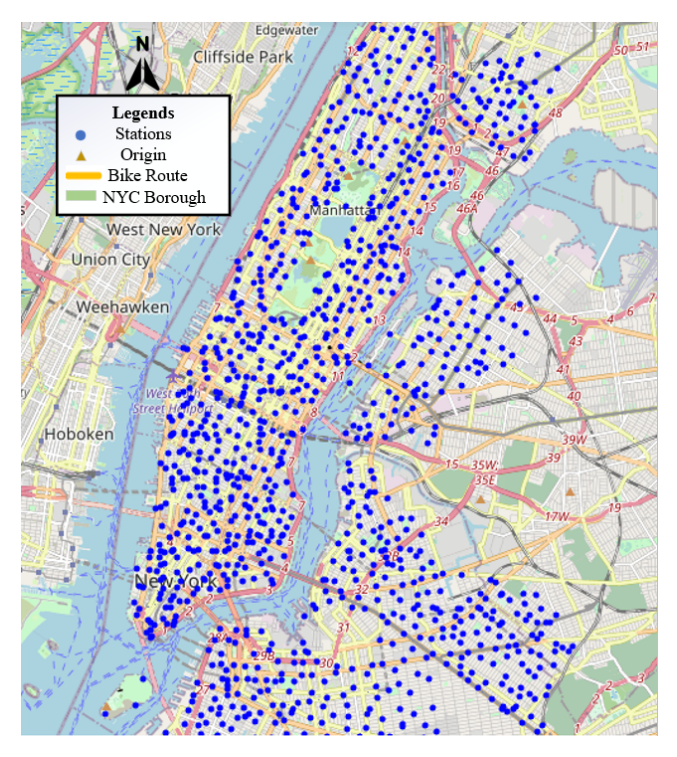


Figure 12: Distribution of Bike stations of NYC (Citibike)

NYC Data: We are considering the bike trip transaction data from March to August 2020 which consist of 9556704 records. The bike dataset consist of Influence factors such as bike data, number of stations, weekdays and weekends. All the BSS data in New York City from January, 2020 to current time can be downloaded from https://ride.citibikenyc.com/system-data. The statistics of the corresponding data-set is described in Table2. In Fig.12, we illustrate origin and destination trips from random citibike dock stations, to analyze the number of trips received from the starting dock stations. Here, we present bike mobility

modelling method for predicting bike demands during weekdays and weekends from different stations at any given time.

Table 2: Information of Bike dataset

Influence Factors	Variables
Bike Data	(March - August 2020)
No. of Records	9556704
No. of Stations	1054
No. of weekdays	130
No. of weekends	53

6.2. Bike Sharing Usage Patterns:

In this section, we develop a Sliced Spatial Heatmap generated from the dataset to demonstrate the spatio-temporal patterns of bike sharing usage as shown in Fig.13.It provides the bike usage demand patterns from morning, afternoon and evening hours of NYC (citibike). It can be observed that the bike usage is concentrated towards the Lower Manhattan downtown location surrounding area of metro-stations, showing the intensity of peak bike demand between (6:00-9:00 and 12:00-15:00) in the daytime and (22:00-24:00) in the evening time respectively.

7. Results and Discussion

7.1. Bike Mobility Prediction Process

In this section, we present the bike mobility modelling method to predict the bike demands across different stations of New-York Citi-bike sharing system. The description of the bike data-set used for the prediction analysis is shown in Table2. In Fig14, we show the distribution demand usage throughout weekdays and weekends respectively. From the bike demand usage pattern, we can interpret that a bigger radius of red circle represents more trips are received by the corresponding bike stations in that location thereby creating high demand of bikes as compared to the locations near the blue circle regions. For, prediction analysis we have considered the bike sharing dataset from March till

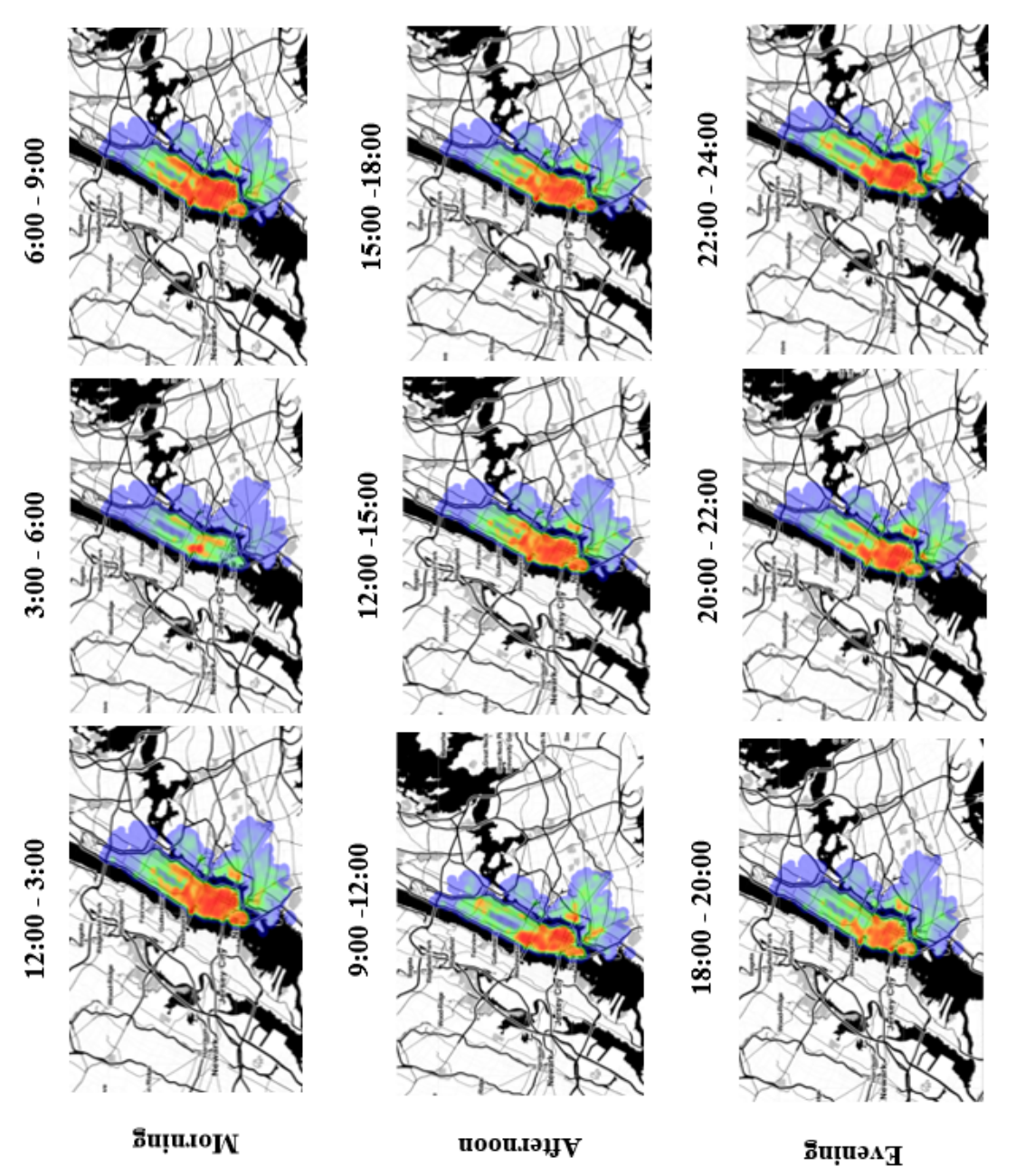


Figure 13: Heat-Map Depicting Spatio-Temporal Pattern of Bike Demand

August, 2020(including both weekdays and weekends). The average bike count demand across all the stations and during the weekdays and weekend is shown in Fig 15.

During our initial analysis, we studied that bike usage trends to investigate the time-series of bike usage data during the entire period of time. The Fig15(a) shows adequate difference in the bike trend usage in all the months that were considered. To, study the variation in the bike trend, we have proposed individual prediction models for both weekdays and weekends bike prediction analysis.

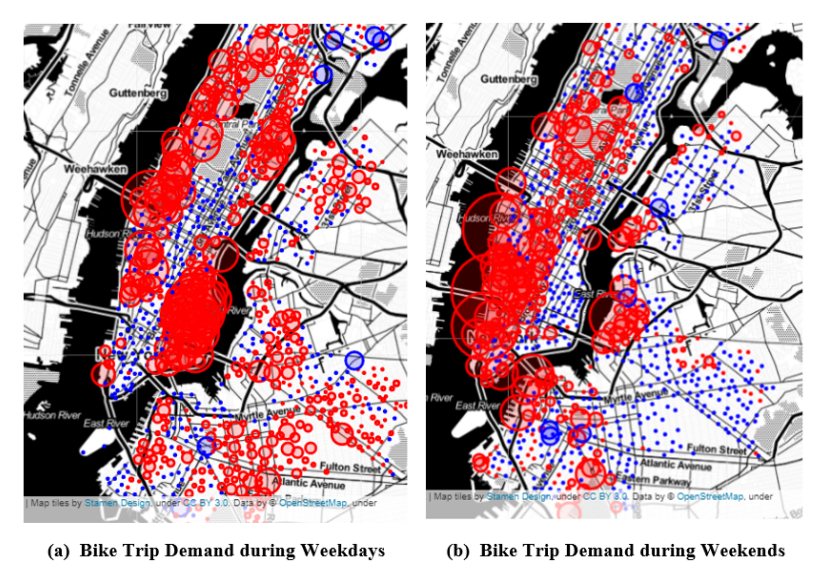


Figure 14: Maximum Bike Demand Stations during Weekdays and Weekends

In Fig.16 we have explained the step-by-step procedure for bike prediction analysis. Using the analysis pipeline, we have considered forecasting approaches such as LSTM and GPR models by applying performance parameters like Mean Square Error (MAE) and Root Mean Square Error (RMSE). In prediction analysis, we have proposed ensemble predictions of LSTM and GPR models, and associated the prediction through discretized weighting method.

In the ensemble approach, we have used LSTM and GPR models using their RMSE and MSE scores as the selection criteria. From the individual prediction models, the discretized weighted approach can be used to obtain the overall

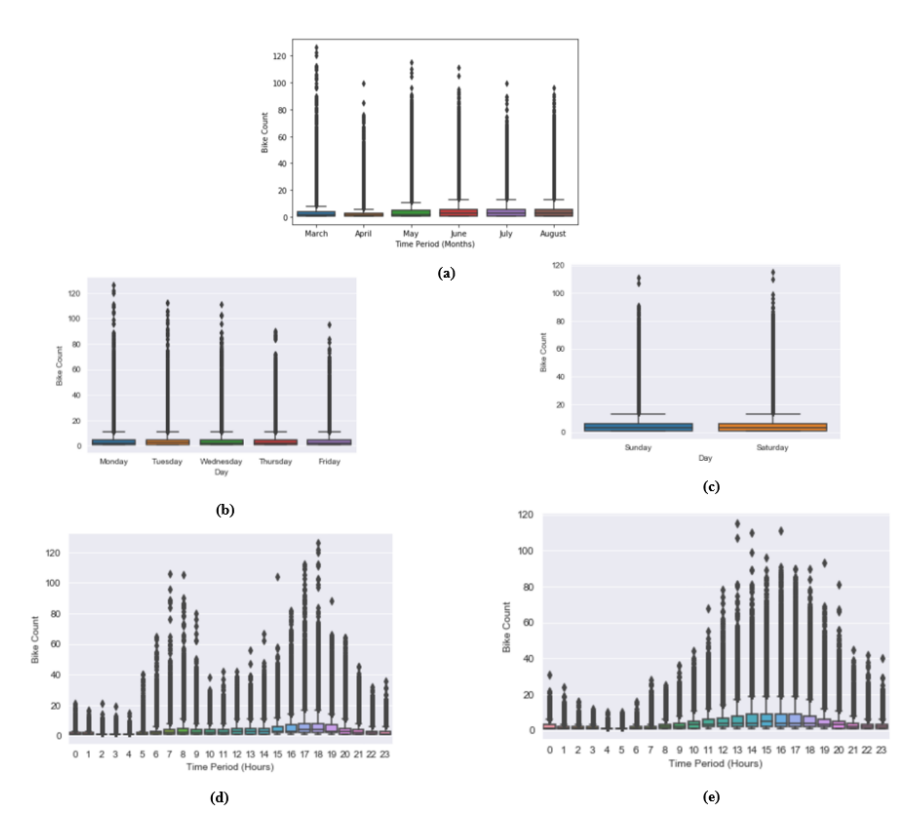


Figure 15: (a):Average Bike Count during each Month; (b):Average Bike count during Weekdays; (c):Average Bike count during Weekends; (d):Hourly Bike count during Weekdays; (e):Hourly Bike count during Weekends

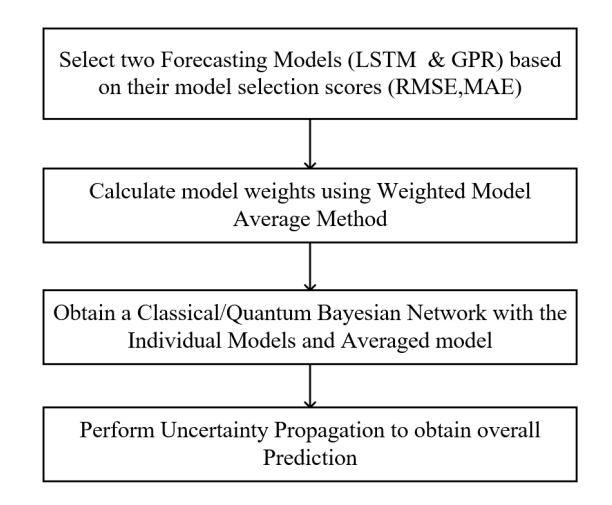


Figure 16: Analysis Pipeline

prediction at a given time, t is shown in Eq. 30

$$Z_t = W_A * Z_{t,A} + W_B * Z_{t,B} \tag{30}$$

Where, $Z_{t,A}$ and $Z_{t,B}$ denote predictions of LSTM and GPR. W_A and W_B denotes weights corresponding to LSTM and GPR models.

$$W_A + W_B = 1 \tag{31}$$

The true values of the predictions are compared with the individual predictions to derive the weights, W_A and W_B . In, developing the prediction model we have considered the bike dataset from (March - July), 2020 as the training data set using LSTM and GPR prediction models and August 2020 as the testing dataset respectively. For the analysis, bike station-id: 72 (52 street and 11 Avenue) is investigated for predicting the bike demand trends.

The LSTM and GPR model performs uncertainty propagation to obtain the overall prediction from the model parameters. From the Eq. 31, we obtain the individual weights and the average predictions of the models respectively. The overall predictions depend on the probability distribution of the model parameters and the weights associated with the models (LSTM and GPR). Since the predictions from both the individual and average predictions are probabilistic, we have proposed probabilistic models such as the Bayesian network for the uncertainty propagation approach. Fig. 17 illustrates the Bayesian network model for average prediction for bike demands.

The following hyperparameters where selected during the empirical analysis. For the LSTM model, with the dropout rate at 0.2, and the initial learning rate at 0.01, the Adam optimizer provided the best-case results and showed a good convergence rate when the training epochs were increased between 500 to 700 epochs. However, for the GPR model, we used the radial basis function kernel to define the covariance function, the amplitude parameter (p_1) at 2, and the length scale parameters (p_2) at 1 provided considerable good results during the

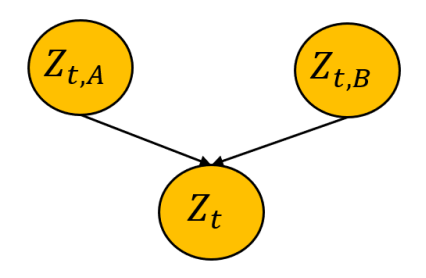


Figure 17: Bayesian network for prediction

training process. The corresponding model performance metrics of LSTM and GPR are shown in Table.3 and Table.4

Table 3: Weekday Model Parameters

S.No	Model	MAE	RMSE	R^2
1	LSTM	2.151	2.959	0.88
2	GPR	3.447	4.688	0.83

Table 4: Weekend Model Parameters

S.No	Model	MAE	RMSE	R^2
1	LSTM	1.674	2.734	0.92
2	GPR	4.255	5.803	0.80

Since QBN are quantum equivalent to the classical version of the Bayesian network. It is possible to perform uncertainty propagation on a quantum computing platform that improves the computational performance of classical algorithms (such as Bayesian networks) (Woerner and Egger, 2019). The underlying drawback in QBN is in presenting complex Bayesian network models with several parent and child nodes.

However, we can counteract this issue by solving one part of the problem using classical Bayesian modelling and the consecutive part by QBN. In this paper, we have solved the individual and weighted model predictions using classical approach, (BN) and the average predictions using quantum approach, (QBN). For instance, the predictions that we obtained from LSTM and GPR models were continuous variables, in order to convert the continuous variables to discrete variables, we have assigned values to the respective states of the qubits that are

required for constructing the Quantum Bayesian Network. In Table.5, we have divided the values into four categories corresponding to four intervals of the two qubits. The four intervals are $|00\rangle$, $|01\rangle$, $|10\rangle$, $|11\rangle$, which represents the states of the $Z_{t,A}$, $Z_{t,B}$ as shown in Fig.17 respectively.

Table 5: Discretized Values for Qubits

States	Range	Value
$ 00\rangle$	(0 - 6)	0
$ 01\rangle$	(6 - 12)	1
$ 10\rangle$	(12 - 18)	2
$ 11\rangle$	(18 - 24)	3

7.1.1. Constructing Quantum Circuit:

From Fig. 15 (d),(e) we can analyze that the bike demand fluctuates every hour. For instance, there is a huge influx in bike demand in the morning hours of weekdays and afternoon hours of weekends. Thereby, the discretized values of the variables is represented in time (hours). As shown in Table.5, the bike demand is divided into four interval periods. The four interval periods are depicted as two-qubit system as $|00\rangle$, $|01\rangle$, $|10\rangle$, $|11\rangle$. The Bayesian network with three nodes $(Z_{t,A}, Z_{t,B}, \text{ and } Z_t)$ is transformed into the quantum Bayesian network as shown in Fig. 18. The transformation U-gates, U_A and U_B represents the probability of nodes $Z_{t,A}$ and $Z_{t,B}$. Hence, the resulting probability of Z_t will have a total of 16 combinations (four values for both $Z_{t,A}$ and $Z_{t,B}$), and the probability of Z_t is illustrated using controlled U-gate.

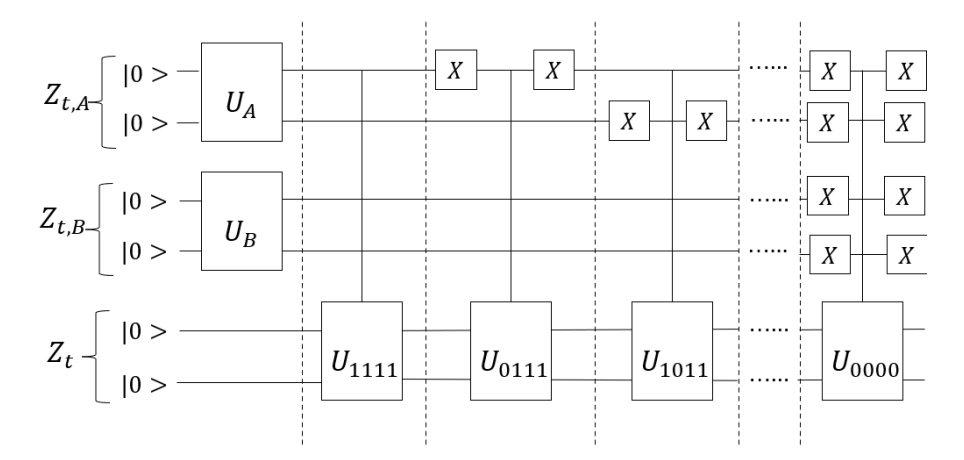


Figure 18: QBN circuit of three-node network Harikrishnakumar et al. (2020)

In this quantum circuit $Z_{t,A}$ represents the parent node, and $Z_{t,B}$ represents the child node. Now, let us assume the probability of four states $|00\rangle, |01\rangle, |10\rangle, |11\rangle$ as $p_{ij}, i=0,1$ and j=0,1. We adopt the decomposition method as mentioned in Section 5 to fragment the U-gate of the root node. The Fig. 8 illustrates the decomposition approach 8, where $R_y(\theta_A)$ is simulated such that the first qubit is $|0\rangle$ and $|1\rangle$ states. The rotation angle of the qubits is calculated using the Eq. 29 as shown below:

$$R_y(\theta) = 2 \times \tan^{-1} \sqrt{\frac{p_{10} + p_{11}}{p_{00} + p_{01}}}.$$
 (32)

Where, rotation angle is calculated when the qubit $|1\rangle$ is represented in both $|10\rangle$ and $|11\rangle$ and qubit $|0\rangle$ in $|00\rangle$ and $|01\rangle$ states of the two-qubit system. In the case, where the state $|1\rangle$ is in first qubit level, then the corresponding second qubit will be in state $|0\rangle$ or $|1\rangle$. To, obtain the probability of the second qubit level we apply CR_y gate as shown in (Fig. 8) respectively.

After, implementing the CR_y gate when the qubit is in state $|0\rangle$ and $|1\rangle$. The decomposition method is used to decompose the U_A and U_B gates. In Fig. 17 Z_t represents the child node, where the conditional gates depends on the values of parent nodes. The conditional gates are fragmented into single gates. This is accomplished using dummy qubits or ancilla qubits as shown in Fig. 9.

Finally, the developed QBN is simulated to derive the probability of Z_t based on the probability of $Z_{t,A}$ and $Z_{t,B}$.

7.1.2. Quantum Circuit Simulation for Weekday and Weekend Scenario:

After, the construction of QBN, the circuit is simulated in the IBM-Qiskit platform for weekday and weekend bike prediction analysis. The simulation analysis thereby measures the respective quantum states ($|100010\rangle$)) as shown in histogram Fig.19. The OBN circuit is simulated for 8192 shots or iterations, which represents the possible number of iterations that can be performed on an actual quantum device (Mandviwalla et al., 2018).

In the experimental case study, we have considered three node Bayesian network (Fig.17), which represents a 6-qubit system with a total of (2⁶) 72-states. The variables $Z_{t,A}$, $Z_{t,B}$, and Z_t are mapped to qubits $|q_9q_8q_3q_2q_1q_0\rangle$ and $|q_4q_5q_6q_7\rangle$ correspond to ancilla qubits or dummy qubits. The probability corresponding to states ($|q_9q_8q_3q_2q_1q_0\rangle$) is calculated as shown below:

$$P(|q_9q_8q_3q_2q_1q_0\rangle) = \frac{|q_9q_8q_3q_2q_1q_0\rangle}{T}$$
 (33)

Where, T represents total number of states, in our case analysis (T =72) respectively. The conditional or marginal probabilities of the three nodes is obtained using the Eq.34.

$$P(|q_i\rangle) = \sum_{q_j, j=9, 8, 3, 2, 1, 0, j \neq i} P(|q_9q_8q_3q_2q_1q_0\rangle)$$
(34)

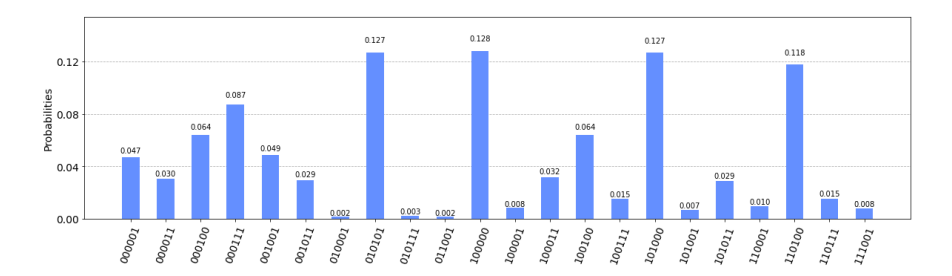


Figure 19: IBM-Qiskit simulation of QBN $\,$

7.1.3. Comparison of Results for Weekday and Weekend Scenario:

(a) Performance comparison: To validate and measure the difference between the classical results and quantum results from Netica and Qiskit is calculated using Eq.35.

$$RMSPE = \epsilon_T = 100\% \sqrt{\sum_i \frac{(p_i - q_i)^2}{4}}$$
 (35)

Where, p_i represents the true value obtained from Netica, q_i are the expectation values from the IBM-Qiskit simulator. To validate the experiment analysis we perform the validation across a weekday and weekend during the month of August to compare the final prediction results obtained from the classical and Quantum computations. For both scenarios we have chosen two-time windows, during the morning and evening hours of bike station id: (72) to determine the final prediction from Qiskit simulator and classical analysis.

(b) Weekday and Weekend Bike demand Forecasting Analysis:

In our work, the main focus is forecasting station-level demand, where bike station-id: 72 (52 street and 11 Avenue) is investigated for forecasting the bike demand trends. In the evaluation study for forecasting bike demand, we simulated a 3-node Bayesian network as shown in 17 on IBM-Qiskit simulator, and compared the results using classical analysis performed in Netica (Netica, 2019). The states $Z_{t,A}$, $Z_{t,B}$ correspond to four intervals of two qubits which provides the forecasted range of bikes during every interval as shown in Table 5.

From the discretized values obtained from the states, we calculate the probabilities of weekday and weekend bike forecasting for the month of August as shown in Table 6 and 7. Based on the spatial-temporal heat map in Fig.13 two-time windows during morning and evening time slots were considered to forecast the bike demands. The analysis for weekday at 9:00 AM state 1 provided the forecasted number of (6-12) bikes that need to be supplied to the bike station during the respective time period, with a 67% accuracy from classical analysis and 66% accuracy from the quantum analysis and, state 2 provided the

forecasted number of (12-18) bikes with 33% accuracy from classical analysis and 34% from the quantum analysis. However, at 9:00 PM state 0 showed the forecast for (0-6) bikes with a 25% accuracy from classical analysis and 24% accuracy from the quantum analysis, state 1 showed the forecast for (6-12) bikes with a 25% accuracy from classical analysis and 23% accuracy from the quantum analysis, state 2 showed the forecast for (12-18) bikes with a 25% accuracy from classical analysis and 26% accuracy from the quantum analysis, state 3 showed the forecast for (18-24) bikes with a 25% accuracy from classical analysis and 27% accuracy from the quantum analysis respectively. Likewise, the marginal probabilities from Qiskit and classical analysis were evaluated for weekend bike forecasting.

From the results obtained, we can observe that the results from the QBN using the Qiskit simulator are almost similar to the results from the classical analysis. The error rate (RMSPE) calculated were within 2% interval for the weekday and weekend bike prediction analysis for the entire day period (24 hours) as shown in Fig.20. Thereby, validating the applicability of QBN for providing effective and accurate bike demand forecasting with computational speed up when compared to the classical Bayesian model. The Appendix A provides the quantum circuit corresponding to BN in Fig.17 developed for weekday and weekend bike forecasting analysis.

Table 6: Values of Marginal Probabilities Compared with Qiskit and Classical Analysis for Weekday Bike Forecasting

Day	Time	State	Netica	QBN	RMSPE			
		state 0	0.0	0.0				
	9:00 AM	state 1	0.67	0.66	0.7			
	9.00 AW	state 2	0.33	0.34	0.7			
8/3/2020		state 3	0.0	0.0				
0/3/2020		state 0	0.25	0.24				
	9:00 PM	state 1	0.25	0.23	1.6			
	9.00 1 M	state 2 0.25 0.		0.26	1.0			
		state 3	0.25	0.27				

 $\hbox{ Table 7: Values of Marginal Probabilities Compared with Qiskit and Classical Analysis for Weekend Bike Forecasting } \\$

Day	Time	State	Netica	QBN	RMSPE		
		state 0	0.0	0.0			
	9:00 AM	state 1	0.45	0.43	1.41		
	9.00 AM	state 2	0.55	0.57	1.41		
8/8/2020		state 3	0.0	0.0			
0/0/2020		state 0	0.0	0.0			
	9:00 PM	state 1	0.83	0.84	0.7		
	9.00 1 W	state 2	0.17	0.16	0.7		
		state 3	0.0	0.0			

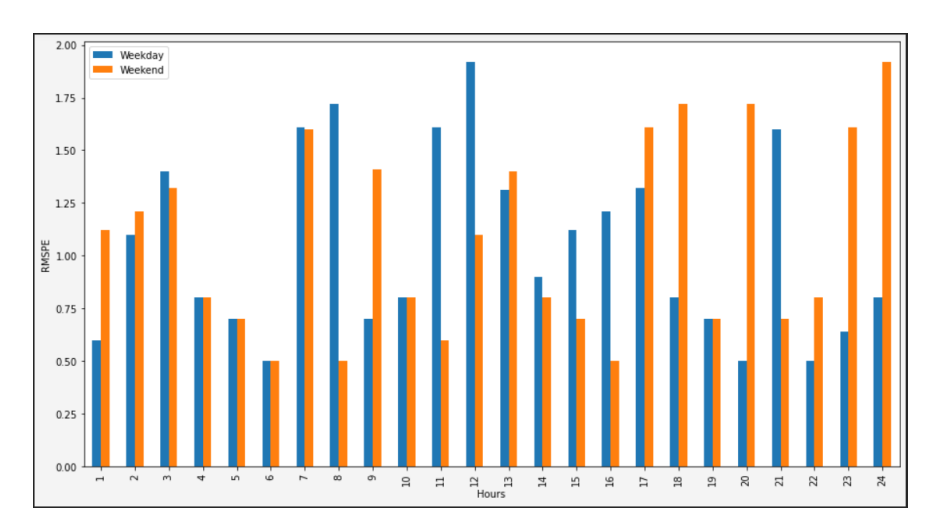


Figure 20: Bar plots associated with RMSPE of the Bike Predictions on Weekdays and Weekends on Qiskit.

8. Conclusion & Future Work

This paper proposed a considered model averaging approach for bike demand prediction at bike sharing system. This paper demonstrated the application of time series forecasting models such as the neural network-based LSTM model and Gaussian process model. The individual predictions from these models are averaged using QBN approach. The weights corresponding to the individual models are calculated as being inversely proportional to their root mean squared errors (RMSE). We demonstrated the QBN approach for model averaging and efficient predictions. This paper demonstrated the proposed approach for bike demand prediction across both weekdays and weekends using NYC Citi Bike data. This paper also compared the prediction performance of the Quantum Bayesian networks against classical Bayesian networks and the RMSPE values were within 2%. For future work, we will also investigate the solution performance when implemented on quantum hardware. Since quantum hardware solution performance is affected by hardware noise and errors, we will also investigate quantum error correction (QEC) techniques to further improve solution performance.

9. Acknowledgements

The research reported in this paper was supported by funds from the National Science Foundation (NSF Grant Number: 2105342). The support is gratefully acknowledged.

References

Ai, Y., Li, Z., Gan, M., Zhang, Y., Yu, D., Chen, W., Ju, Y., 2018. A deep learning approach on short-term spatiotemporal distribution forecasting of dockless bike-sharing system. Neural Computing and Applications 31, 1665– 1677.

- Ajagekar, A., Humble, T., You, F., 2020. Quantum computing based hybrid solution strategies for large-scale discrete-continuous optimization problems. Computers & Chemical Engineering 132, 106630.
- Alfailakawi, M.G., Ahmad, I., Hamdan, S., 2016. Harmony-search algorithm for 2d nearest neighbor quantum circuits realization. Expert Systems with Applications 61, 16–27.
- Bergholm, V., Izaac, J., Schuld, M., Gogolin, C., Alam, M.S., Ahmed, S., Arrazola, J.M., Blank, C., Delgado, A., Jahangiri, S., et al., 2018. Pennylane: Automatic differentiation of hybrid quantum-classical computations. arXiv preprint arXiv:1811.04968.
- Borujeni, S.E., Nannapaneni, S., Nguyen, N.H., Behrman, E.C., Steck, J.E., 2021. Quantum circuit representation of bayesian networks. Expert Systems with Applications 176, 114768. URL: https://www.sciencedirect.com/science/article/pii/S0957417421002098, doi:https://doi.org/10.1016/j.eswa.2021.114768.
- Boushaki, S.I., Kamel, N., Bendjeghaba, O., 2018. A new quantum chaotic cuckoo search algorithm for data clustering. Expert Systems with Applications 96, 358–372.
- Caggiani, L., Camporeale, R., Ottomanelli, M., Szeto, W.Y., 2018. A modeling framework for the dynamic management of free-floating bike-sharing systems. Transportation Research Part C: Emerging Technologies 87, 159–182. URL: https://www.sciencedirect.com/science/article/pii/S0968090X18300020, doi:https://doi.org/10.1016/j.trc.2018.01.001.
- Cantelmo, G., Kucharski, R., Antoniou, C., 2020. Low-dimensional model for bike-sharing demand forecasting that explicitly accounts for weather data. Transportation Research Record: Journal of the Transportation Research Board 2674, 036119812093216. doi:10.1177/0361198120932160.

- Chai, D., Wang, L., Yang, Q., 2018. Bike flow prediction with multi-graph convolutional networks, in: GIS: Proceedings of the ACM International Symposium on Advances in Geographic Information Systems, pp. 397–400. doi:10.1145/3274895.3274896, arXiv:1807.10934.
- Chen, P.C., Hsieh, H.Y., Sigalingging, X.K., Chen, Y.R., Leu, J.S., 2017. Prediction of Station Level Demand in a Bike Sharing System Using Recurrent Neural Networks, in: IEEE Vehicular Technology Conference, pp. 1–5. doi:10.1109/VTCSpring.2017.8108575.
- Dallaire-Demers, P.L., Wilhelm, F.K., 2016. Quantum gates and architecture for the quantum simulation of the fermi-hubbard model. Physical Review A 94, 062304.
- Dokuz, A.S., 2021. Fast and efficient discovery of key bike stations in bike sharing systems big datasets. Expert Systems with Applications 172, 114659.
- El-Assi, W., Salah Mahmoud, M., Nurul Habib, K., 2017. Effects of built environment and weather on bike sharing demand: a station level analysis of commercial bike sharing in toronto. Transportation 44, 589–613.
- Erdoğan, G., Laporte, G., Calvo, R.W., 2014. The static bicycle relocation problem with demand intervals. European Journal of Operational Research 238, 451–457.
- Gammelli, D., Peled, I., Rodrigues, F., Pacino, D., Kurtaran, H.A., Pereira, F.C., 2020. Estimating latent demand of shared mobility through censored gaussian processes. Transportation Research Part C: Emerging Technologies 120, 102775. URL: https://www.sciencedirect.com/science/article/pii/S0968090X20306859, doi:https://doi.org/10.1016/j.trc.2020.102775.
- Gammelli, D., Wang, Y., Prak, D., Rodrigues, F., Minner, S., Pereira, F.C., 2022. Predictive and prescriptive performance of bike-sharing demand fore-

- casts for inventory management. Transportation Research Part C: Emerging Technologies 138, 103571.
- Gao, C., Chen, Y., 2022. Using machine learning methods to predict demand for bike sharing, in: Information and Communication Technologies in Tourism 2022: Proceedings of the ENTER 2022 eTourism Conference, January 11–14, 2022, Springer. pp. 282–296.
- Goodfellow, I.J., Bengio, Y., Courville, A., 2016. Deep Learning. MIT Press, Cambridge, MA, USA. http://www.deeplearningbook.org.
- Gyongyosi, L., Imre, S., 2019. Quantum circuit design for objective function maximization in gate-model quantum computers. Quantum Information Processing 18, 1–33.
- Harikrishnakumar, R., Borujeni, S.E., Ahmad, S.F., Nannapaneni, S., 2021.
 Rebalancing bike sharing systems under uncertainty using quantum bayesian networks, in: 2021 IEEE International Conference on Quantum Computing and Engineering (QCE), IEEE. pp. 461–462.
- Harikrishnakumar, R., Borujeni, S.E., Dand, A., Nannapaneni, S., 2020. A quantum bayesian approach for bike sharing demand prediction, in: 2020 IEEE International Conference on Big Data (Big Data), pp. 2401–2409. doi:10.1109/BigData50022.2020.9378271.
- He, T., Bao, J., Li, R., Ruan, S., Li, Y., Tian, C., Zheng, Y., 2018. Detecting vehicle illegal parking events using sharing bikes' trajectories, in: Proceedings of the ACM SIGKDD International Conference on Knowledge Discovery and Data Mining, pp. 340–349. doi:10.1145/3219819.3219887.
- Hochreiter, S., Schmidhuber, J., 1997. Long short-term memory. Neural computation 9, 1735–1780.
- Hulot, P., Aloise, D., Jena, S.D., 2018. Towards station-level demand prediction for effective rebalancing in bike-sharing systems, in: Proceedings of the ACM

- SIGKDD International Conference on Knowledge Discovery and Data Mining, pp. 378–386. doi:10.1145/3219819.3219873.
- Kadowaki, T., Nishimori, H., 1998. Quantum annealing in the transverse Ising model. Physical Review E - Statistical Physics, Plasmas, Fluids, and Related Interdisciplinary Topics doi:10.1103/PhysRevE.58.5355, arXiv:9804280.
- Kaltenbrunner, A., Meza, R., Grivolla, J., Codina, J., Banchs, R., 2010. Urban cycles and mobility patterns: Exploring and predicting trends in a bicycle-based public transport system. Pervasive and Mobile Computing 6, 455–466. URL: https://www.sciencedirect.com/science/article/pii/S1574119210000568, doi:https://doi.org/10.1016/j.pmcj.2010.07.002. human Behavior in Ubiquitous Environments: Modeling of Human Mobility Patterns.
- Kaspi, M., Raviv, T., Tzur, M., 2016. Detection of unusable bicycles in bikesharing systems. Omega-international Journal of Management Science 65, 10–16.
- Kopczyk, D., 2018. Quantum machine learning for data scientists. arXiv preprint arXiv:1804.10068.
- Krizek, K.J., Stonebraker, E.W., 2011. Assessing options to enhance bicycle and transit integration. Transportation Research Record doi:10.3141/2217-20.
- Lenton, T.M., Held, H., Kriegler, E., Hall, J.W., Lucht, W., Rahmstorf, S., Schellnhuber, H.J., 2008. Tipping elements in the Earth's climate system. doi:10.1073/pnas.0705414105.
- Li, X., Xu, Y., Zhang, X., Shi, W., Yue, Y., Li, Q., 2023. Improving short-term bike sharing demand forecast through an irregular convolutional neural network. Transportation Research Part C: Emerging Technologies 147, 103984.
- Li, Y., Zhu, Z., Kong, D., Xu, M., Zhao, Y., 2019. Learning heterogeneous

- spatial-temporal representation for bike-sharing demand prediction, in: Proceedings of the AAAI conference on artificial intelligence, pp. 1004–1011.
- Lin, L., He, Z., Peeta, S., 2018. Predicting station-level hourly demand in a large-scale bike-sharing network: A graph convolutional neural network approach. Transportation Research Part C: Emerging Technologies 97, 258-276. URL: https://www.sciencedirect.com/science/article/pii/ S0968090X18300974, doi:https://doi.org/10.1016/j.trc.2018.10.011.
- Liu, K., Hu, X., Wei, Z., Li, Y., Jiang, Y., 2019a. Modified gaussian process regression models for cyclic capacity prediction of lithium-ion batteries. IEEE Transactions on Transportation Electrification 5, 1225–1236. doi:10.1109/ TTE.2019.2944802.
- Liu, X., Gherbi, A., Li, W., Cheriet, M., 2019b. Multi features and multitime steps lstm based methodology for bike sharing availability prediction. Procedia Computer Science 155, 394–401.
- Liu, Z., Shen, Y., Zhu, Y., 2018. Inferring dockless shared bike distribution in new cities. Proceedings of the Eleventh ACM International Conference on Web Search and Data Mining.
- Low, G.H., Yoder, T.J., Chuang, I.L., 2014. Quantum inference on bayesian networks. Physical Review A 89, 062315.
- Ma, X., Yin, Y., Jin, Y., He, M., Zhu, M., 2022. Short-term prediction of bikesharing demand using multi-source data: a spatial-temporal graph attentional lstm approach. Applied Sciences 12, 1161.
- Mandviwalla, A., Ohshiro, K., Ji, B., 2018. Implementing grover's algorithm on the ibm quantum computers, in: 2018 IEEE International Conference on Big Data (Big Data), IEEE. pp. 2531–2537.
- McKay, D.C., Alexander, T., Bello, L., Biercuk, M.J., Bishop, L., Chen, J., Chow, J.M., Córcoles, A.D., Egger, D., Filipp, S., et al., 2018. Qiskit back-

- end specifications for open qasm and open pulse experiments. arXiv preprint ${\rm arXiv:}1809.03452$.
- Mehdizadeh Dastjerdi, A., Morency, C., 2022. Bike-sharing demand prediction at community level under covid-19 using deep learning. Sensors 22, 1060.
- Moreira, C., Wichert, A., 2016. Quantum-like bayesian networks for modeling decision making. Frontiers in psychology 7, 11.
- Netica, 2019. Norsys software corporation, netica version 6.05. https://www.norsys.com/.
- Nielsen, M.A., Chuang, I., 2002. Quantum computation and quantum information. American Association of Physics Teachers.
- Nikiforiadis, A., Ayfantopoulou, G., Stamelou, A., 2020. Assessing the impact of covid-19 on bike-sharing usage: The case of thessaloniki, greece. Sustainability 12. URL: https://www.mdpi.com/2071-1050/12/19/8215, doi:10.3390/su12198215.
- Osaba, E., Villar-Rodriguez, E., Oregi, I., 2022. A systematic literature review of quantum computing for routing problems. IEEE Access .
- Ozsoydan, F.B., Baykasoğlu, A., 2019. Quantum firefly swarms for multimodal dynamic optimization problems. Expert Systems with Applications 115, 189–199.
- Pan, Y., Zheng, R.C., Zhang, J., Yao, X., 2019. Predicting bike sharing demand using recurrent neural networks. Procedia Computer Science 147, 562-566. URL: https://www.sciencedirect.com/science/article/pii/S1877050919302364, doi:https://doi.org/10.1016/j.procs.2019.01.217. 2018 International Conference on Identification, Information and Knowledge in the Internet of Things.
- Phillipson, F., Neumann, N., Wezeman, R., 2022. Classification of hybrid quantum-classical computing. arXiv preprint arXiv:2210.15314.

- Qiskit Community, 2017. Qiskit: An open-source framework for quantum computing. URL: https://github.com/Qiskit/qiskit, doi:10.5281/zenodo. 2562110.
- Ramesh, A.A., Nagisetti, S.P., Sridhar, N., Avery, K., Bein, D., 2021. Station-level demand prediction for bike-sharing system, in: 2021 IEEE 11th Annual Computing and Communication Workshop and Conference (CCWC), IEEE. pp. 0916–0921.
- Rasmussen, C.E., Nickisch, H., 2010. Gaussian processes for machine learning (gpml) toolbox. The Journal of Machine Learning Research 11, 3011–3015.
- Santos, A.C., 2016. The ibm quantum computer and the ibm quantum experience. arXiv preprint arXiv:1610.06980.
- Sathishkumar, V., Park, J., Cho, Y., 2020. Using data mining techniques for bike sharing demand prediction in metropolitan city. Computer Communications 153, 353–366.
- She, L., Han, S., Liu, X., 2021. Application of quantum-like bayesian network and belief entropy for interference effect in multi-attribute decision making problem. Computers & Industrial Engineering 157, 107307. URL: https://www.sciencedirect.com/science/article/pii/S0360835221002114, doi:https://doi.org/10.1016/j.cie.2021.107307.
- Singhvi, D., Singhvi, S., Frazier, P.I., Henderson, S.G., O'Mahony, E., Shmoys, D.B., Woodard, D.B., 2015. Predicting bike usage for new york city's bike sharing system., in: AAAI Workshop: Computational Sustainability, pp. 1–5.
- Tucci, R.R., 1995. Quantum bayesian nets. International Journal of Modern Physics B 9, 295–337.
- VE, S., Cho, Y., 2020. A rule-based model for seoul bike sharing demand prediction using weather data. European Journal of Remote Sensing 53, 166–183.

- Villwock-Witte, N., van Grol, L., 2015. Case Study of Transit-Bicycle Integration. Transportation Research Record: Journal of the Transportation Research Board doi:10.3141/2534-02.
- Wang, B., Kim, I., 2018. Short-term prediction for bike-sharing service using machine learning. Transportation research procedia 34, 171–178.
- Woerner, S., Egger, D.J., 2019. Quantum risk analysis. npj Quantum Information 5, 1–8.
- Xiao, G., Wang, R., Zhang, C., Ni, A., 2020. Demand prediction for a public bike sharing program based on spatio-temporal graph convolutional networks. Multimedia Tools and Applications doi:10.1007/s11042-020-08803-y.
- Xie, N., Li, Z., Liu, Z., Tan, S., 2023. A censored semi-bandit model for resource allocation in bike sharing systems. Expert Systems with Applications 216, 119447.
- Xin-gang, Z., Ji, L., Jin, M., Ying, Z., 2020. An improved quantum particle swarm optimization algorithm for environmental economic dispatch. Expert Systems with Applications 152, 113370.
- Yang, Y., Heppenstall, A., Turner, A., Comber, A., 2019. A spatiotemporal and graph-based analysis of dockless bike sharing patterns to understand urban flows over the last mile. Computers, Environment and Urban Systems 77, 101361.
- Yang, Y., Heppenstall, A., Turner, A., Comber, A., 2020. Using graph structural information about flows to enhance short-term demand prediction in bikesharing systems. Computers, Environment and Urban Systems 83, 101521.
- Yu, L., Feng, T., Li, T., Cheng, L., 2022. Demand prediction and optimal allocation of shared bikes around urban rail transit stations. Urban Rail Transit, 1–15.

- Zaltz Austwick, M., O'Brien, O., Strano, E., Viana, M., 2013. The structure of spatial networks and communities in bicycle sharing systems. PloS one 8, e74685.
- Zeng, M., Yu, T., Wang, X., Su, V., Nguyen, L.T., Mengshoel, O.J., 2016. Improving demand prediction in bike sharing system by learning global features, in: KDD 2016, pp. 10–18.
- Zhang, J., Zheng, Y., Qi, D., 2017. Deep spatio-temporal residual networks for citywide crowd flows prediction, in: Thirty-first AAAI conference on artificial intelligence, p. 00.
- Zhong, C., Arisona, S.M., Huang, X., Batty, M., Schmitt, G., 2014. Detecting the dynamics of urban structure through spatial network analysis. International Journal of Geographical Information Science 28, 2178–2199.

Appendix A. Quantum circuit for Weekday and Weekend scenario

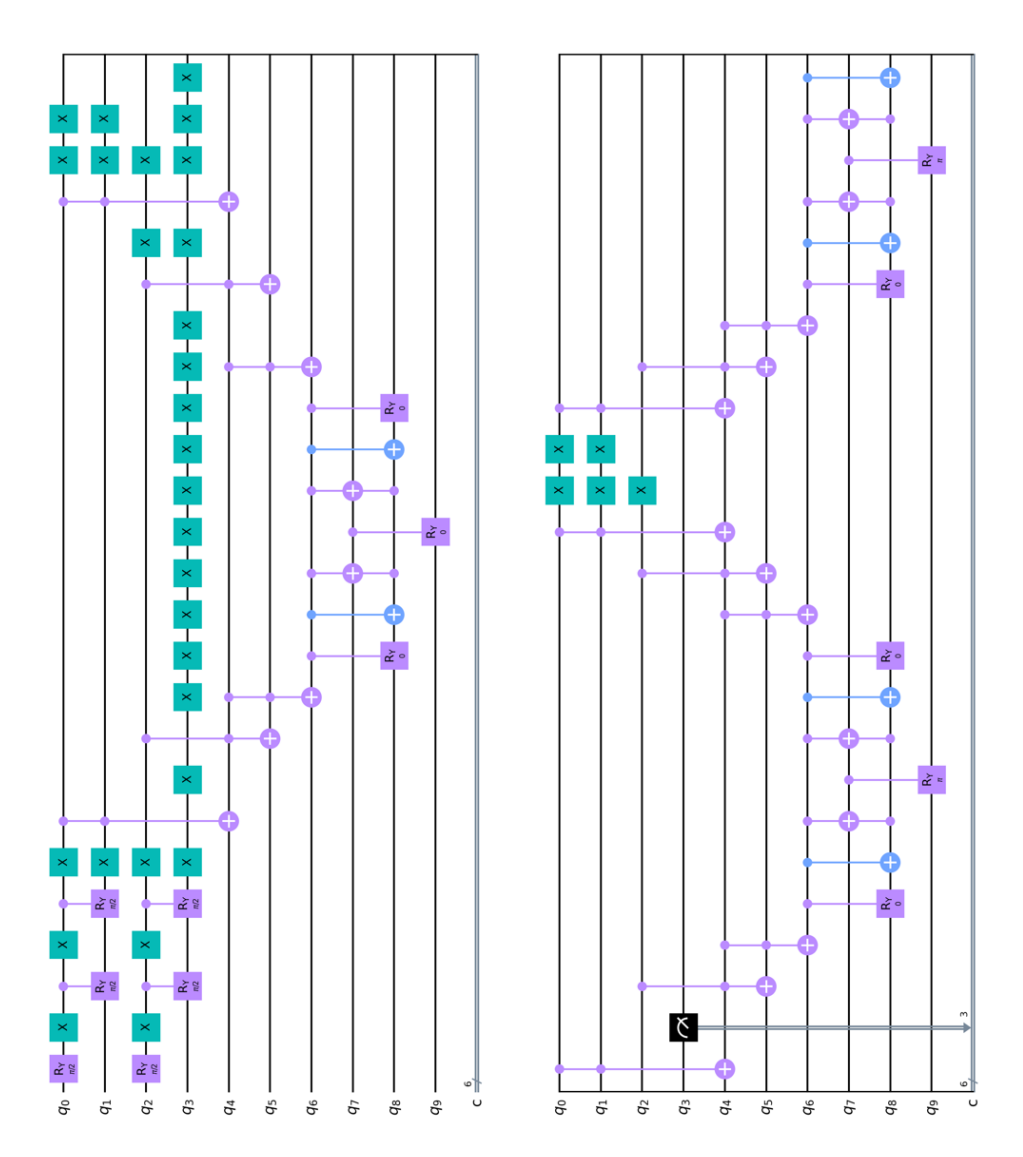


Figure A.21: QBN of the three-node circuit. Nodes $(Z_{t,A}, Z_{t,B} \text{ and } Z_t)$ are mapped to q_9, q_8, q_3, q_2, q_1 , and q_0 respectively, and q_4, q_5, q_6 and q_7 are the ancilla qubits.

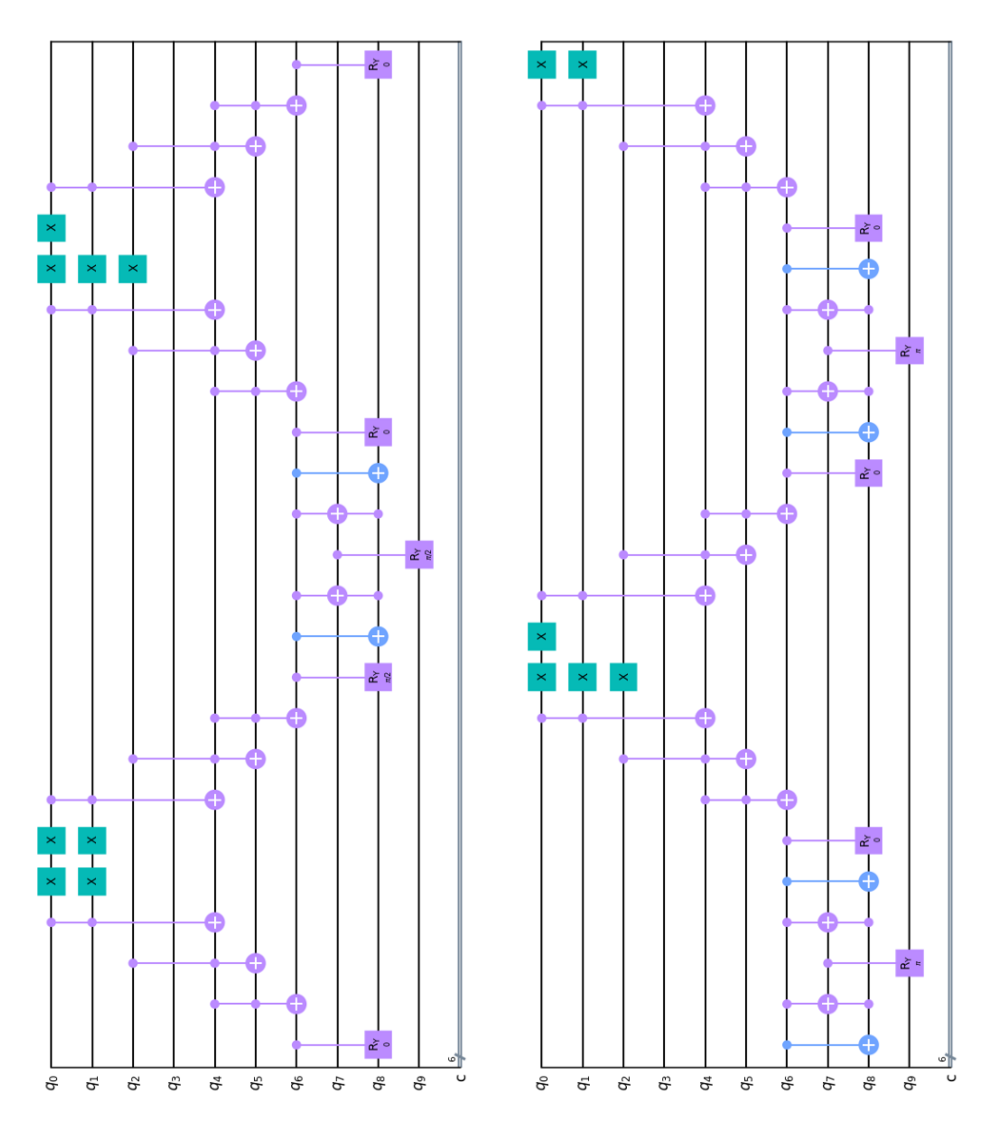


Figure A.21: QBN of the three-node circuit. Nodes $(Z_{t,A}, Z_{t,B} \text{ and } Z_t)$ are mapped to q_9, q_8, q_3, q_2, q_1 , and q_0 respectively, and q_4, q_5, q_6 and q_7 are the ancilla qubits. (contd)

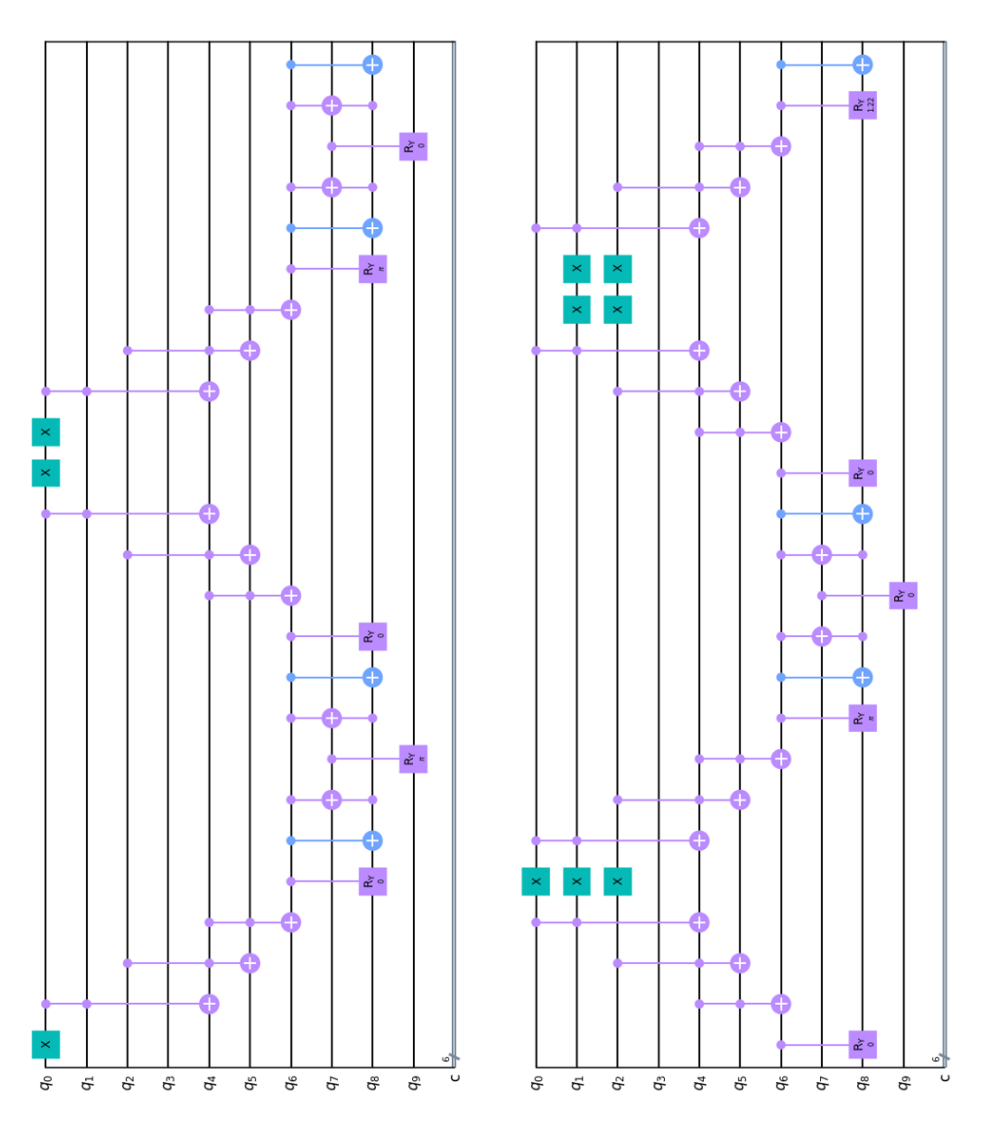


Figure A.21: QBN of the three-node circuit. Nodes $(Z_{t,A}, Z_{t,B} \text{ and } Z_t)$ are mapped to q_9, q_8, q_3, q_2, q_1 , and q_0 respectively, and q_4, q_5, q_6 and q_7 are the ancilla qubits. (contd)

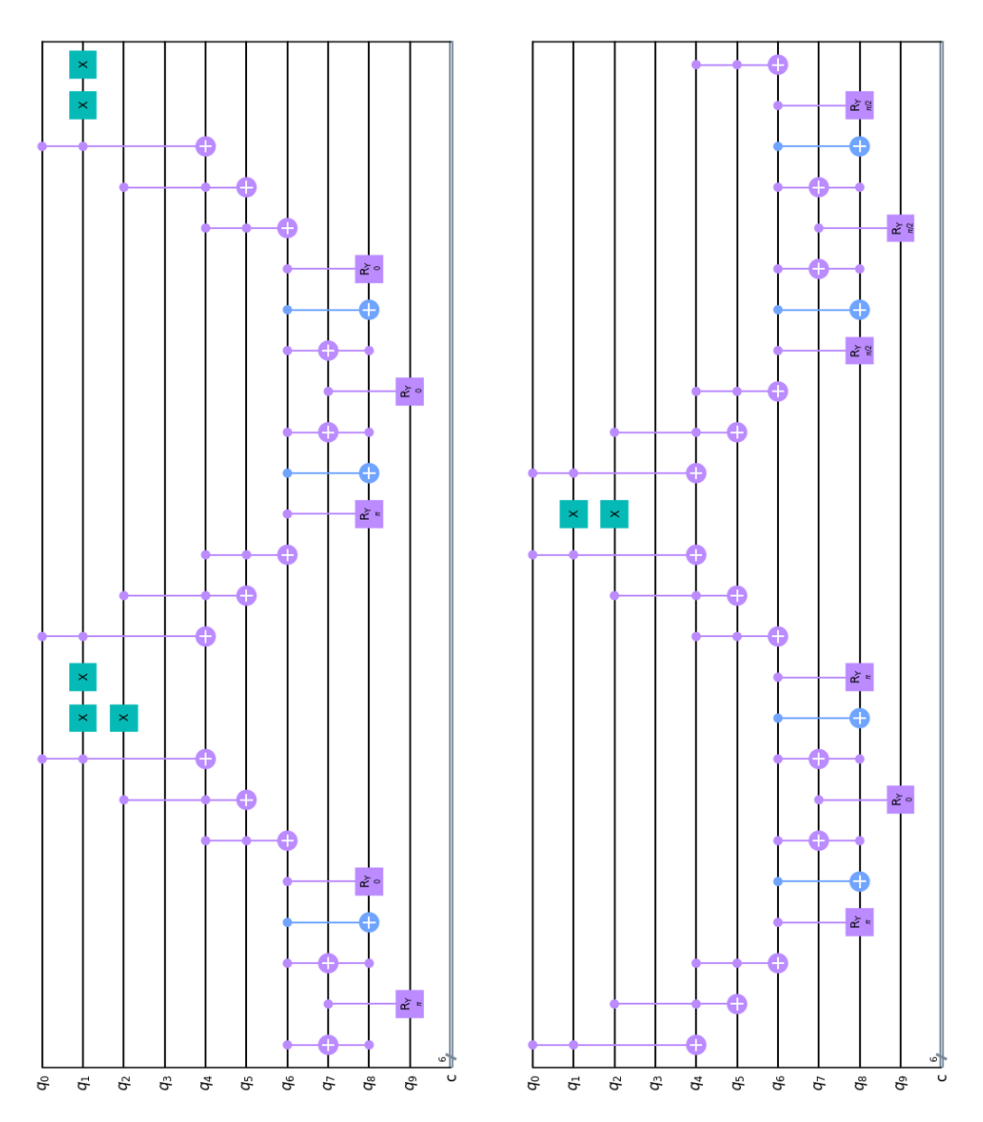


Figure A.21: QBN of the three-node circuit. Nodes $(Z_{t,A},Z_{t,B} \text{ and } Z_t)$ are mapped to $q_9,\,q_8,\,q_3,\,q_2,\,q_1,\,$ and q_0 respectively, and $q_4,\,q_5,\,q_6$ and q_7 are the ancilla qubits. (contd)

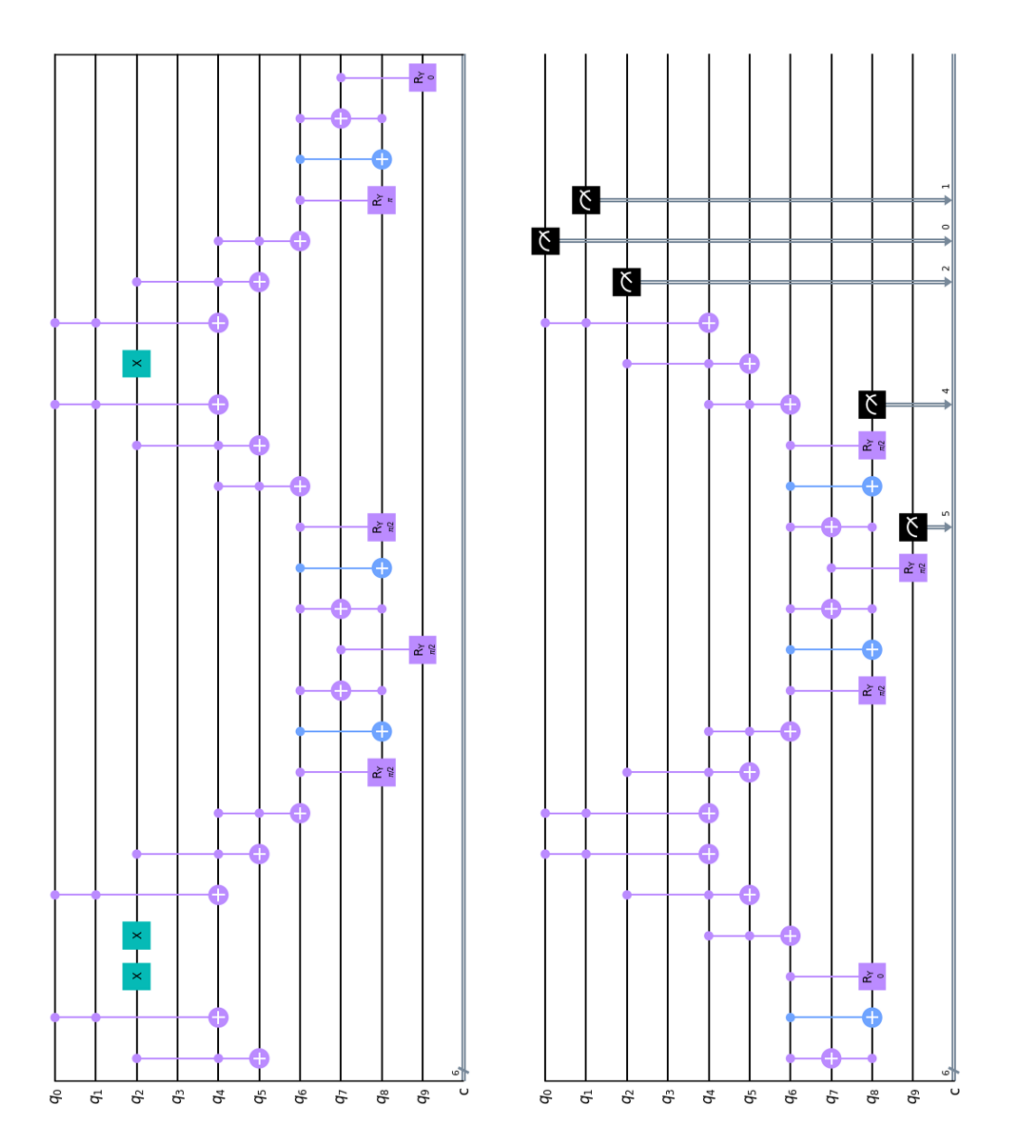


Figure A.21: QBN of the three-node circuit. Nodes $(Z_{t,A}, Z_{t,B} \text{ and } Z_t)$ are mapped to q_9, q_8, q_3, q_2, q_1 , and q_0 respectively, and q_4, q_5, q_6 and q_7 are the ancilla qubits.

CRediT authorship contribution statement

Ramkumar Harikrishnakumar: Conceptualization, Methodology, Software, Formal analysis, Investigation, Data curation, Writing - original draft, Visualization. **Saideep Nannapaneni:** Validation, Investigation, Resources, Writing - review & editing, Supervision, Project administration.

Declaration of interests
\Box The authors declare that they have no known competing financial interests or personal relationships that could have appeared to influence the work reported in this paper.
☑ The authors declare the following financial interests/personal relationships which may be considered as potential competing interests:
Saideep Nannapaneni reports financial support was provided by National Science Foundation.

Highlights

- 1. Propose a novel Quantum Bayesian ensemble approach for bike demand prediction during weekday and weekend scenarios.
- 2. Discretization of the continuous-valued bike demand forecasts to enable the construction of Quantum Bayesian networks.
- 3. Leveraging Quantum Bayesian Network with similar bike usage patterns to enable demand forecasting.